THE JOURNAL OF BIOLOGICAL CHEMISTRY VOL. 287, NO. 34, pp. 28291–28306, August 17, 2012

Methylglyoxal Activates Nociceptors through Transient Receptor Potential Channel A1 (TRPA1)

A POSSIBLE MECHANISM OF METABOLIC NEUROPATHIES[*] [S]

Received for publication, December 5, 2011, and in revised form, May 15, 2012 Published, JBC Papers in Press, June 27, 2012, DOI 10.1074/jbc.M111.328674

Mirjam J. Eberhardt[‡§], Milos R. Filipovic[§], Andreas Leffler[¶], Jeanne de la Roche[¶], Katrin Kistner[‡], Michael J. Fischer[‡], Thomas Fleming[‖], Katharina Zimmermann[‡], Ivana Ivanovic-Burmazovic[§], Peter P. Nawroth[‖], Angelika Bierhaus[‖], Peter W. Reeh[‡], and Susanne K. Sauer[‡1]

From the [‡]Institute of Physiology and Pathophysiology Friedrich-Alexander University Erlangen-Nuremberg, Universitaetsstrasse 17, 91054 Erlangen, Germany, [§]Department of Chemistry and Pharmacy, Friedrich-Alexander University Erlangen-Nuremberg, Egerlandstrasse 1, 91058 Erlangen, Germany, [¶]Department of Anesthesiology and Intensive Care, Medical School Hannover, Carl-Neuberg-Strasse 1, 30625 Hannover, Germany, and [‖]Department of Medicine I and Clinical Chemistry, University Hospital Heidelberg, Im Neuenheimer Feld 410, 69120 Heidelberg, Germany

Background: Methylglyoxal is a reactive metabolite that modifies proteins and accumulates in diabetes and uremia.
Results: Methylglyoxal excites nociceptors and releases neuropeptides via activation of TRPA1 channels by modifying their intracellular N-terminal cysteine and lysine residues.
Conclusion: Methylglyoxal acting through TRPA1 is a possible cause of painful metabolic neuropathies.
Significance: Methylglyoxal and its reaction with TRPA1 are promising targets for medicinal chemistry to fight neurotoxicity.

Neuropathic pain can develop as an agonizing sequela of diabetes mellitus and chronic uremia. A chemical link between both conditions of altered metabolism is the highly reactive compound methylglyoxal (MG), which accumulates in all cells, in particular neurons, and leaks into plasma as an index of the severity of the disorder. The electrophilic structure of this cytotoxic ketoaldehyde suggests TRPA1, a receptor channel deeply involved in inflammatory and neuropathic pain, as a molecular target. We demonstrate that extracellularly applied MG accesses specific intracellular binding sites of TRPA1, activating inward currents and calcium influx in transfected cells and sensory neurons, slowing conduction velocity in unmyelinated peripheral nerve fibers, and stimulating release of proinflammatory neuropeptides from and action potential firing in cutaneous nociceptors. Using a model peptide of the N terminus of human TRPA1, we demonstrate the formation of disulfide bonds based on MG-induced modification of cysteines as a novel mechanism. In conclusion, MG is proposed to be a candidate metabolite that causes neuropathic pain in metabolic disorders and thus is a promising target for medicinal chemistry.

Methylglyoxal (MG)[2] is a reactive intracellular metabolite synthesized as a byproduct in several metabolic pathways but mainly from triose phosphates in glycolysis or from lipid peroxidation (1, 2). MG levels mediate rapid non-enzymatic glycation of proteins and other substrates, promoting formation of advanced glycation end products. MG also appears in the plasma where it is increased in patients suffering from diabetes as hyperglycemia strongly enhances MG accumulation (3). In addition, experimental diabetes models suggest a down-regulation of the MG detoxifying glyoxalase 1 system, leading to a further rise of MG levels (4). In diabetic patients, increased MG plasma levels exceeding 800 nM have been measured (5, 6), implying that considerably higher concentrations should be present intracellularly. The exaggerated glycolytic metabolism resulting from hyperglycemia is known to activate and sensitize primary nociceptive neurons (7–9). Painful neuropathy also occurs in patients suffering from chronic renal failure that also involves elevated plasma levels of MG (6, 10). In this pathological condition, "carbonyl stress" such as by MG has been considered to be responsible for many concomitant complications (11). This makes MG an important cytotoxic metabolite in diseases affecting an increasing number of the aging population and in pathophysiological conditions that are linked to neuropathy and pain. Chemically, MG is a highly reactive ketoaldehyde that reacts with arginine and lysine residues of proteins to form stable adducts and MG-derived lysine-arginine cross-linking structures. MG has also been described to react reversibly with cysteine residues to produce hemithioacetal products (12). Also known as acetyl formaldehyde, MG shares chemical similarity with established agonists of the transient receptor potential (TRP) channel A1 (TRPA1) such as formaldehyde and acrolein.

TRPA1 was first described as an ion channel expressed in sensory neurons that is activated by cold and noxious isothio-

* This work was supported by the Emerging Fields Initiative (*Medicinal Redox Inorganic Chemistry*) of the University of Erlangen-Nuremberg; the Dr. Robert Pfleger-Stiftung (to K. K.); Deutsche Forschungsgemeinschaft Grants BI-1281/3-1 (to A. B.), NA 138/7-1 (to P. P. N.), and LU 728/3-1 (to P. W. R.); and the Dietmar-Hopp-Stiftung (to A. B. and P. P. N.).
[S] This article contains supplemental Figs. 1–3 and Tables 1 and 2.
[1] To whom correspondence should be addressed. Tel.: 49-9131-85-26729; Fax: 49-9131-85-22497; E-mail: sauer@physiologie1.uni-erlangen.de.
[2] The abbreviations used are: MG, methylglyoxal; AITC, allyl isothiocyanate; CAP, compound action potential; CGRP, calcitonin gene-related peptide; DRG, dorsal root ganglion; ESI, electrospray ionization; PLC, phospholipase C; SIF, synthetic interstitial fluid; TRPA1, transient receptor potential channel A1; TRPV1, transient receptor potential channel V1; TRP, transient receptor potential; hTRPA1, human TRPA1; MHC, mechano-, heat-, and cold-sensitive; MH, mechano- and heat-sensitive; 4-HNE, 4-hydroxynonenal.

cyanate compounds (13, 14). Although the role of TRPA1 in cold sensing is still discussed controversially with a growing consensus regarding cold hyperalgesia, it has well been established that many endogenous mediators and metabolites act through TRPA1. As it is activated by hypoxia (15), CO_2 (16), lactic acid (17), and mediators of oxidative stress (18) and inflammation (19, 20), TRPA1 has increasingly emerged as relevant for nociception and pain in pathophysiological conditions. Recent studies also indicate that TRPA1 may be a promising target for treatment of airway inflammation (21), colitis (22), and diabetes (23, 24).

For activation by many noxious compounds, certain cysteine residues in the N-terminal intracellular domain of the receptor channel are crucial. It has been shown that these cysteine residues are covalently bound and modified by highly reactive electrophilic compounds (25, 26). Recent findings on the structure of mouse TRPA1 reveal a close proximity of these cysteines (26, 27) that is maintained when functional tetramers are formed by TRPA1. This proximity promotes chemical interactions of agonists with the cysteines but also enables reactions of the cysteines with each other, which may modulate channel activation.

The aim of our study was to scrutinize direct effects of MG on TRPA1 receptor channels expressed in primary sensory neurons and transfected cells as well as in isolated tissue preparations. We propose a distinct activation mechanism of TRPA1 by MG. In the N terminus of the receptor, MG activation involves a particular lysine residue and modification of cysteine residues by formation of disulfide bonds. The results suggest a possible role of MG in TRPA1-mediated neuropathic pain that results from severe metabolic disorders.

EXPERIMENTAL PROCEDURES

Mouse Models—TRPA1$^{+/-}$ mice were donated by Harvard University (Drs. Kelvin Kwan and David Corey, Boston, MA) and TRPV1$^{+/-}$ mice were a gift from Glaxo-Smith-Kline (Dr. John Davis, Harlow, UK). Mice were housed under a 12-h light/dark cycle and had free access to food and water. Mice were sacrificed in a pure CO_2 atmosphere before excision of tissues for investigating stimulated CGRP release or culture of dorsal root ganglion (DRG) neurons. All procedures of this study were approved by the animal protection authorities (local district government, Ansbach, Germany).

Isolation of DRGs, DRG Culture, HEK 293t Cell Culture, and Transfection—DRGs of C57Bl/6, congenic TRPA1, or TRPV1 knock-out mice were excised and transferred into Dulbecco's modified Eagle's medium (DMEM) solution containing 50 μg/ml gentamicin (Sigma-Aldrich). As described previously, ganglia were treated with 1 mg/ml collagenase and 0.1 mg/ml protease for 30 min (both from Sigma-Aldrich) and subsequently dissociated using a fire-polished silicone-coated Pasteur pipette (28). The cells were plated on poly-D-lysine-coated (200 μg/ml; Sigma-Aldrich) coverslips and cultured in TNB 100 cell culture medium supplemented with TNB 100 lipid-protein complex (Biochrom, Berlin, Germany), 100 μg/ml streptomycin, penicillin (PAA Laboratories, Pasching, Austria), and 100 ng/ml mouse NGF (Alomone Labs, Tel Aviv, Israel) at 37 °C in 5% CO_2. Calcium imaging experiments were performed within 20–30 h of dissociation.

Human and rat TRPA1 cDNA and cDNA of a mutant human TRPA1 (hTRPA1) lacking lysine and/or cysteine residues in the intracellular domain (C621S/C641S/C665S +/− K710R) were a kind gift from Dr. Sven-Eric Jordt (Department of Pharmacology, Yale University, New Haven, CT). Single mutations of lysine 710 to arginine or glutamine and a C621S/C641S/C665S/K710Q hTRPA1 mutant were generated by site-directed mutagenesis using the QuikChange II XL kit (Agilent Technologies, Santa Clara, CA) with modified primer design (29) and confirmed by sequencing. HEK 293t cells were transfected with plasmids of hTRPA1, rat TRPA1, or mutant hTRPA1 (1 μg each) using Nanofectin (PAA Laboratories, Pasching, Austria). For patch clamp recordings, cells were co-transfected with 0.5 μg of GFP cDNA. After incubation for 24 h, cells were plated on coated coverslips and used for experiments the same day.

Assessment of Intracellular MG—For detection of intracellular MG, DRGs (20–24 each) of four C57Bl/6 mice were prepared as described above and pooled. The freshly dissociated neurons were split to give at least 4000 cells/ml for each sample used for establishing standard curves and determining MG contents with or without MG exposure. The suspended cells were counted using an automated cell counter (Scepter, Millipore), which also provides a readout of the approximate volume of the counted cells, thus allowing calculation of concentration. Cells were incubated with two different concentrations of MG (1 μM and 3 mM) for 12 h or just 90 s, respectively, washed, and then lysed by sonication. Intracellular MG measurement was performed using 1,2-diaminobenzene as described previously (30). An UltiMate 3000 (Dionex) UHPLC equipped with a photodiode array detector was used. Samples were eluted on a PLRP-S polymeric reversed phase column (250 × 4.6 mm, Zorbax, Poroshell) with a flow rate of 0.5 ml/min using 32% acetonitrile and 68% 10 mM NaH_2PO_4, pH 2.5 as a mobile phase. This method was shown to measure free, unbound MG and possibly MG released from hemithioacetals but does not detect stable MG adducts to lysine or arginine residues in proteins (30).

Whole-cell Voltage Clamp Recordings—Whole-cell voltage clamp was performed on transfected HEK 293t cells. Membrane currents were acquired with an EPC10 USB HEKA amplifier (HEKA Elektronik, Lamprecht, Germany), low passed at 1 kHz, and sampled at 2 kHz. Electrodes were pulled from borosilicate glass tubes (TW150F-3, World Precision Instruments, Berlin, Germany) and heat-polished to give a resistance of 1.5–3.0 megaohms. The standard external solution contained 140 mM NaCl, 5 mM KCl, 2 mM $MgCl_2$, 5 mM EGTA, 10 mM HEPES, and 10 mM glucose, pH 7.4 (adjusted with tetramethyl-ammonium hydroxide). In some experiments, EGTA was replaced by 2 mM $CaCl_2$ as noted. The internal solution contained 140 mM KCl, 2 mM $MgCl_2$, 5 mM EGTA, and 10 mM HEPES, pH 7.4 (adjusted with KOH). If not otherwise noted, cells were held at −60 mV. For current-voltage curves with and without methylglyoxal, currents were measured during 500-ms-long voltage ramps from −100 to +100 mV. All experiments were performed at room temperature. Solutions were applied with a gravity-driven polytetrafluoroethylene-glass multibarrel perfusion system. Patchmaster/Fitmaster software (HEKA Elektronik, Lambrecht/Pfalz, Germany) was used for acquisition and off-line analysis.

Ratiometric $[Ca^{2+}]_i$ Measurements—Cells were stained by 5 μM fura-2/AM and 0.02% Pluronic (both from Invitrogen) for about 30 min. Following a 30-min washout period to allow for fura-2/AM ester hydrolysis, coverslips were mounted on an Olympus IX71 inverse microscope with a 10× (HEK 293t cells) or 20× (DRGs) objective. Cells were constantly superfused with extracellular fluid (145 mM NaCl, 5 mM KCl, 1.25 mM $CaCl_2$, 1 mM $MgCl_2$, 10 mM glucose, and 10 mM HEPES) using a software-controlled seven-channel gravity-driven common outlet superfusion system. Fura-2 was excited at 340 and 380 nm with a Polychrome V monochromator (Till Photonics, Gräfelfing, Germany). Images were exposed for 2 ms and acquired at a rate of 1 Hz with a 12-bit charge-coupled device camera (Imago Sensicam QE, Till Photonics). Data were recorded and further analyzed using TILLvisION 4.0.1.3 software (Till Photonics). Background was subtracted before calculation of ratios. A 60 mM potassium (DRGs) or 10 μM ionomycin stimulus (HEK 293t cells) was applied as a control at the end of each experiment. The area under the curve of F340/380 nm ratios was quantified for regions of interest adapted to the neurons.

Biochemical Characterization of MG-induced Modification of hTRPA1—A model peptide of the intracellular N-terminal sequence of hTRPA1 comprising amino acids 607–670 (UniProt accession number O75762; Thermo Fisher Scientific, Schwerte, Germany) was synthesized to evaluate MG effects on cysteines, which have been described to be covalently modified and crucial for TRPA1 activation (25). Ultrahigh resolution ESI-TOF mass spectrometry was performed on a maXis mass spectrometer (Bruker Daltonics, Bremen, Germany) on 50 μM peptide in 20 mM ammonium bicarbonate buffer, pH 7.4, which was treated with 500 μM methylglyoxal for 15 min and then sprayed directly into the ion source. The instrumental parameters were as follows: injection rate, 180 μl/h; source temperature, 320 °C; capillary voltage, 4.5 kV; collision voltage, 10 kV.

Measurement of CGRP Release—The skin from both hind paws or sciatic and vagus nerves were harvested from adult C57Bl/6, TRPA1, or TRPV1 knock-out mice after sacrificing mice in a pure CO_2 atmosphere. The skin flaps were subcutaneously excised below the knee and tied around acrylic glass rods with the corium side exposed (28). The vagus nerves were dissected after removing the submandibular gland and the sternohyoid muscle, transected at the level of the carotid bifurcation, and tracked caudally to the outlet of the recurrent laryngeal nerve where each vagus was excised, and its sheath was removed under binocular control (31). Sciatic nerves were excised from their origin at the lumbar plexus to their branching into tibial, sural, and peroneal nerves and desheathed (32). The preparations were washed for 30 min in carbogen-gassed (95% O_2 and 5% CO_2) synthetic interstitial fluid (SIF (33)) containing 108 mM NaCl, 3.48 mM KCl, 3.5 mM $MgSO_4$, 26 mM $NaHCO_3$, 1.7 mM NaH_2PO_4, 1.5 mM $CaCl_2$, 9.6 mM sodium gluconate, 5.5 mM glucose, and 7.6 mM sucrose. Experiments were performed at 32 or 37 °C for paw skin or sciatic and vagus nerves, respectively.

After washout, the preparations were first incubated twice for 5 min in test tubes containing SIF to determine basal CGRP release. This was followed by 5-min incubation in tubes containing solutions of MG dissolved in SIF for chemical stimulation and a final 5-min incubation period in SIF to assess reversibility of stimulated CGRP release. Blockers or sensitizers of TRPA1 receptors were added from the second to the fourth incubation period. The used incubation fluid was recovered and stored on ice, and the CGRP content of the incubation fluid was measured using a commercial enzyme immunoassay kit (Bertin Pharma, Montingy le Bretonneux, France) with a detection limit of 2 pg/ml. The antibodies used are directed against human α/β-CGRP but are 100% cross-reactive against mouse CGRP. The enzyme immunoassay plates were analyzed photometrically using a microplate reader (Dynatech, Channel Islands, UK). For column diagrams reflecting an increase in stimulated CGRP, base-line levels were subtracted from CGRP values obtained from 5-min stimulation periods.

Compound Action Potential (CAP) Recordings from C- and A-fibers of Isolated Mouse Sciatic Nerves—CAP recordings were made from C- and A-fibers of isolated mouse sciatic nerves (34). Nerves from C57Bl/6 and TRPA1 knock-out mice were prepared as described above and mounted in a three-compartment chamber where they were continuously superfused with SIF at a rate of 5–7 ml/min at 37 °C. Each end of the nerve was threaded into one of two side chambers sealed by a perforated rubber foil and filled with fluorocarbon oil FC-43 (3 M, Neuss, Germany) and placed on a pair of gold wire electrodes. One chamber contained the differential recording electrode, whereas the other was used for electrical stimulation. To monitor the entire population of sciatic nerve axons activated by electrical stimulation, the CAP was evoked by 25% supramaximal electrical stimulation with constant voltage pulses (A395, World Precision Instruments, Sarasota, FL) of 0.1-ms duration at a rate of 0.2 Hz and recorded with a monopolar electrode. After a 20-min control period in SIF, the effects of methylglyoxal (10 mM) applied for 20 min on both latency and peak to peak amplitude of C- and A-fiber CAPs were assessed. The amplitude was taken between the maximum and minimum excursions of the recorded waveform. Latency was assessed as the delay after which a trigger level in the lower third of the CAP upstroke was exceeded. Data were acquired and analyzed using a CED Micro1401 and Spike2 software (Cambridge Electronic Design, UK).

Single Fiber Electrophysiology of the Skin Nerve Preparation—Single fiber recordings of identified primary afferents from skin of C57Bl/6 and TRPA1 knock-out mice were carried out using the skin nerve preparation *in vitro* as has been described previously (28, 35). Briefly, after sacrificing mice by exposure to a pure CO_2 atmosphere, the saphenous nerve was dissected downward from the upper thigh and excised together with the hairy skin of the dorsal hind paw and lower leg containing its receptive fields. The skin was pinned to the bottom of an organ chamber with the corium side exposed, and the cut nerve was pulled through a hole into a separate recording chamber where it was placed on a small mirror. Under binocular control, fine filaments were teased from the desheathed nerve until single fiber activity could be recorded through a monopolar gold wire electrode, which was isolated in a layer of paraffin oil. The skin preparation was continuously superfused with carbogen-saturated SIF, pH 7.4 at 30 °C.

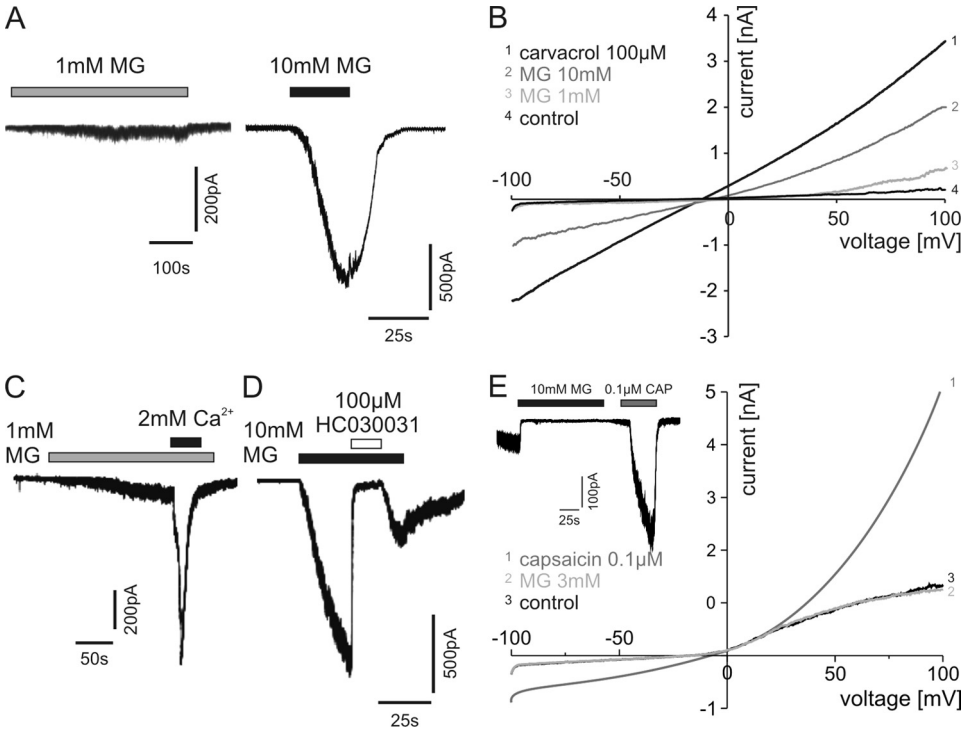

FIGURE 1. **MG activates human TRPA1.** *A*, representative inward currents in HEK 293t cells expressing hTRPA1 at 1 and 10 mM MG. Cells were held at −60 mV. *B*, ramp currents through TRPA1 in calcium-free extracellular solution (control) and during application of 1 or 10 mM MG. Activation of TRPA1 by 100 µM carvacrol is shown as a control. Cells were held at −60 mV, and currents were measured during voltage ramps from −100 to +100 mV within 500 ms. *C*, a typical MG-induced inward current was highly increased by switching from calcium-free to external solution containing 2 mM calcium. *D*, the TRPA1 antagonist HC030031 (100 µM) completely blocked MG-evoked inward currents. *E*, no changes in conductance were observed in rat TRPV1-expressing HEK 293t cells under 3 mM MG in contrast to capsaicin (0.1 µM). Furthermore, MG did not induce inward currents in concentrations up to 10 mM in capsaicin-responsive cells (*E*, *inset*).

Receptive fields of single fibers were searched by probing the corium side of the skin with a blunt glass rod. Conduction velocity was determined using electrical stimulation of fibers in their receptive field with a Teflon-coated steel microelectrode (impedance, 1 megaohm). Mechanical (von Frey) thresholds were determined by means of gravity-driven filaments with uniform blunt 0.9-mm-diameter tips delivering forces in the range of 1–256 mN. For determination of heat or cold responsiveness of the fibers or application of 10 mM methylglyoxal, the receptive fields were isolated using a metal cylinder and petroleum jelly. Within the so-formed chamber, the receptive field could be cooled down (8 °C for 60 s) or heated up (to 47 °C within 20 s) with a separate superfusion system. The temperature was constantly recorded using a thermocouple. Data were sampled and analyzed with the DAPSYS data acquisition system 8.

Statistics—Data are displayed as mean ± S.E. Within one experimental group, data were compared by the Wilcoxon matched pair test or between groups using the Mann-Whitney *U* test. Multiple groups were compared by analysis of variance followed by the Tukey post hoc test with Statistica 7 software (StatSoft, Tulsa, OK). Differences were considered significant at $p < 0.05$ (marked with *).

RESULTS

Methylglyoxal in Mouse DRG Neurons—To estimate the potentially effective intracellular concentration achieved by extracellular application of different MG concentrations as well as by different exposure periods in cultured mouse DRG neurons, a method was used that detects unbound MG and MG reversibly bound as hemithioacetal but not stable MG adducts of lysine and arginine residues in proteins (see below and Ref. 30). In a sample of freshly dissociated native DRG neurons (~3.5×10^4 cells), an intracellular MG concentration of 1.5 µM was detected. In samples exposed to MG, intracellular levels were increased. Treatment for 90 s with 3 mM MG (as in calcium microfluorometric experiments) resulted in about the same intracellular increase to 2.2 µM as exposure to 1 µM for 12 h, implying that the apparent diffusion barrier can be overcome with time possibly due to the fact that a large part of the intracellular MG is at least loosely bound to proteins.

Methylglyoxal Activates Human TRPA1—To investigate whether MG exhibits TRPA1 agonistic properties, HEK 293t cells expressing wild type hTRPA1 were examined by standard whole-cell voltage clamp. Whereas 1 mM MG induced only small inward currents in these cells, activation at 10 mM MG was immediate, leading to large inward currents (Fig. 1*A*; $V_h = -60$ mV). MG also induced concentration-dependent inward currents in HEK 293t cells transfected with rat TRPA1 (not shown). MG was effective in 20% ($n = 14$) of these cells at a 1 mM concentration and activated 100% of cells at 3 and 10 mM ($n = 13$ and 8, respectively). Measuring ramp currents by depolarization from −100 to +100 mV, 1 and 10 mM MG induced an increase in conductance of hTRPA1 (Fig. 1*B*). Carvacrol (100 µM), which has been shown to activate TRPA1 (36), was used as

a control. Extracellular calcium at 2 mM strongly potentiated 1 mM MG-induced inward currents (Fig. 1*C*), which has been described for other TRPA1 agonists (37, 38). Furthermore, TRPA1 antagonist HC030031 (100 μM) completely blocked inward currents evoked by 10 mM MG (Fig. 1*D*). To examine whether TRPV1 may also be activated by MG as has been described for other TRPA1 agonists at high concentrations such as mustard oil (39), HEK 293t cells were transfected with rat TRPV1. MG at 10 mM did not induce inward currents in these cells ($n = 5$), whereas application of 0.1 μM capsaicin led to their immediate activation (Fig. 1*E*, *inset*). In contrast to capsaicin, application of 10 mM MG also did not change the conductance of rat TRPV1-expressing HEK 293t cells (Fig. 1*E*).

Activation of Sensory Neurons by MG Involves Modification of Intracellular Cysteines of TRPA1—To extend the mechanistic insight into the effects of MG, ratiometric calcium signals were measured in native DRG neurons of C57Bl/6 mice. MG applied at a concentration of 3 mM for 90 s evoked robust increases of intracellular calcium as shown for the mean of 72 responding cells and in pseudocolored images from representative experiments (Fig. 2*A*, *upper panel*, and *B*). For control of functional TRP receptor expression, the TRPA1 agonist mustard oil (100 μM AITC for 20 s) and the TRPV1 agonist capsaicin (0.3 μM for 10 s) were applied at 7-min intervals after the MG stimulus. Notably, AITC but not capsaicin activated the same subpopulation of neurons as MG (Fig. 2*B*). The MG-evoked increase in intracellular calcium could be completely prevented by HC030031 (50 μM; Fig. 2, *A* and *C*) and by calcium-free external solution and was also absent in DRGs of TRPA1 knock-out mice (Fig. 2*A*). Following application of MG, the area under the curve of intracellular calcium responses to AITC was 0.03 $\pm$ 0.01, which is significantly diminished compared with the AITC-evoked responses after washout of MG and HC030031 (area under the curve, 0.13 $\pm$ 0.01) or MG in calcium-free solution (area under the curve, 0.16 $\pm$ 0.01; analysis of variance $F(2,229) = 21.2$; honestly significant difference post hoc test, both $p < 0.001$). The percentage of DRGs responding to AITC also decreased by 38% following MG application, which is in agreement with cross-desensitization of TRPA1 following previous receptor activation by MG (40). MG activated DRGs of C57Bl/6 and congenic TRPV1 but not TRPA1 knock-out mice in a concentration-dependent manner as shown by the area under the curve of calcium responses of all MG-treated cells (Fig. 2*D*). Only 1.3% of the neurons responded to a concentration of 300 μM MG, but 55% were activated by 3 mM MG.

To narrow down the binding site of MG, HEK 293t cells were transfected with hTRPA1. In a carvacrol (250 μM for 30 s)-sensitive population, MG applied for 90 s (0.03–10 mM) led to a concentration-dependent increase in the number of activated cells with an EC_{50} of 744 $\pm$ 120 μM (Fig. 2*E*). Interestingly, although higher concentrations of MG activated a larger percentage of hTRPA1-expressing cells, the magnitude of calcium influx was about equal at low and high concentrations as shown for such divergent concentrations as 1 μM and 3 mM MG in supplemental Fig. 1A ($p = 0.163$, *t* test of independent samples). However, the latency of the response was quite variable at 1 μM and longer on average.

To isolate functional MG binding partners in hTRPA1, HEK 293t cells were transfected with the C621S/C641S/C665S mutant (hTRPA1–3C), as the N-terminal cysteines of mouse as well as human TRPA1 have been shown to be essential for gating of the channel by electrophilic compounds (25, 26). In this hTRPA1–3C mutant, the concentration-response curve was shifted rightward to an EC_{50} of 1.8 $\pm$ 0.1 mM (Fig. 2*E*). Interestingly, when MG was applied at 10 mM, a biphasic response similar to that in the wild type occurred (not shown) with a second peak of intracellular calcium shortly after the offset of MG in the early washout period (supplemental Fig. 1B).

Besides cysteines, MG can react with arginine and lysine (12); the latter in position 710 also contributes to hTRPA1 activation. After a single mutation of this lysine residue to glutamine, cells did not respond to MG at concentrations below 3 mM, and the early but not the second peak of MG (10 mM)-induced calcium influx was abolished in these mutants (supplemental Fig. 1B, upper panel). At a lower concentration (1 mM), the MG-evoked calcium transients in the hTRPA1–3C mutant resembled that of the single lysine mutant at 10 mM MG, indicating that MG modification of lysine is responsible for the first peak of MG-evoked responses and accounts for the high concentration effects in the cellular model.

In hTRPA1–3C/K710Q, sensitivity for MG was almost completely lost; only 4 $\pm$ 1.5% of cells responded at 10 mM MG (Fig. 2*E*). MG at 10 mM did not activate untransfected HEK 293t cells. All mutants responded to carvacrol, ensuring hTRPA1 expression and function.

From a biochemical point of view, the properties of lysine are more conserved in arginine than in glutamine. Moreover, lysine to arginine mutants have also been used to study the effects of TRPA1 agonists (25). MG has been described to bind to arginine as well as to lysine (12) but not to glutamine. Indeed, substitution of lysine 710 to arginine either in the single or quadruple mutation resulted in a reduced responsiveness when compared with wild type hTRPA1 (supplemental Fig. 1C). However, substitution of lysine 710 by glutamine resulted in an even stronger abrogation of MG responsiveness as compared with the single or quadruple mutants containing arginine at position 701. Although these data are indicative of a cooperative binding site for MG to activate hTRPA1, the three cysteines might determine the sensitivity of hTRPA1 to 1 mM or lower concentrations of MG.

Biochemical Characterization of the MG-induced Modification of Critical Cysteine Residues in hTRPA1—To further investigate the role of the N-terminal cysteines in the activation by MG, a custom-made synthetic 607–670 peptide comprising the critical cysteine residues but not lysine 710 (Fig. 3*A*) was used as a model system to biochemically characterize the reaction in more detail. The peptide was synthesized and analyzed by ESI-TOF mass spectrometry. Deconvolution of the spectrum revealed a monoisotopic peak of the intact peptide to be at *m*/*z* 7661.50 (calculated *m*/*z*, 7661.53) (supplemental Fig. 1A). After incubation with a 10-fold excess of MG, the reaction mixture was further analyzed by ESI-TOF mass spectrometry. The intact peptide still remained the most abundant peak (supplemental Fig. 1B), but data analysis of the peptide fragments suggested that up to three critical cysteine residues were covalently

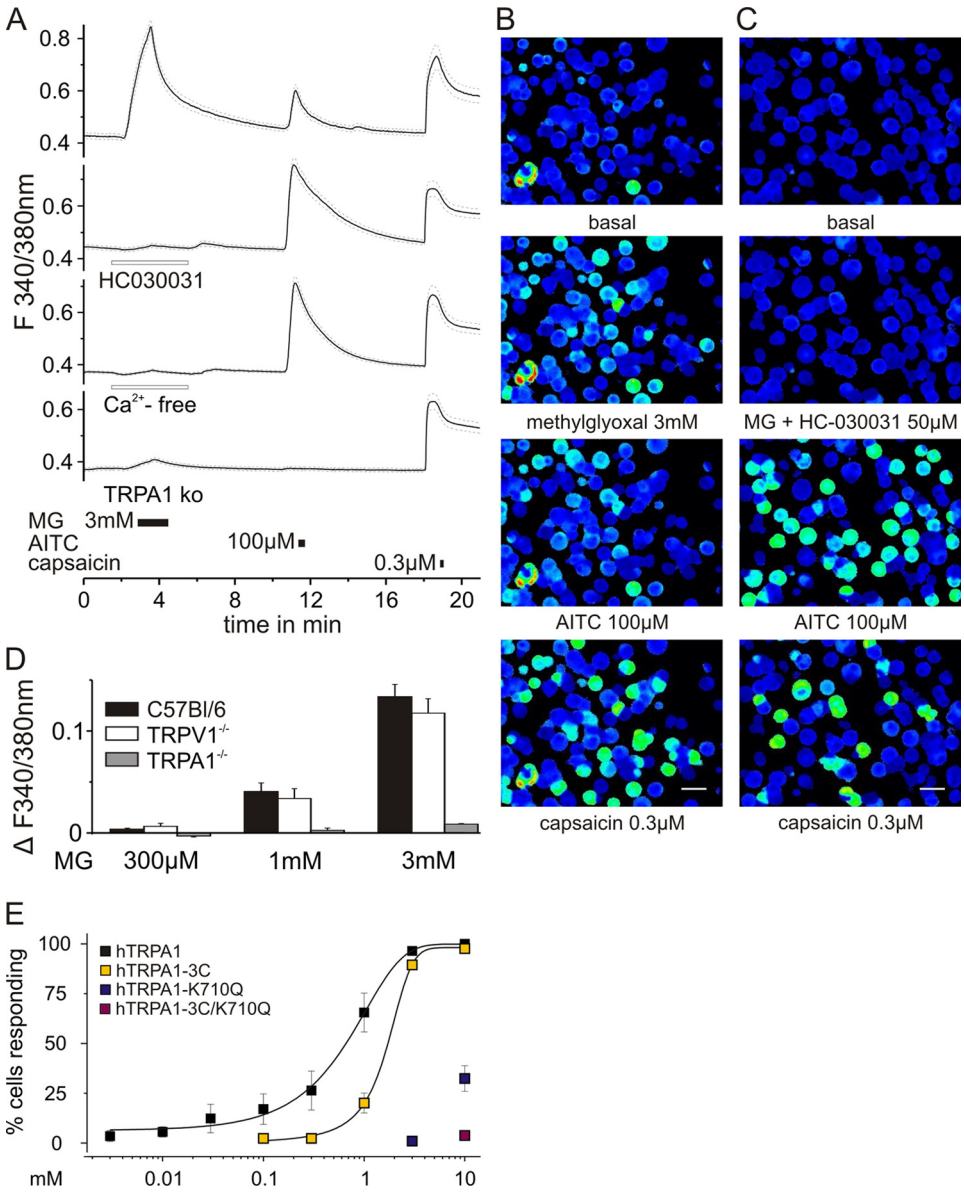

FIGURE 2. **Calcium influx evoked by MG involves modification of intracellular cysteines and lysine residues of TRPA1.** *A*, MG (3 mM) applied for 90 s evoked an increase in intracellular calcium ratiometrically measured in fura-2-stained DRG neurons ($n = 72$; 53.3%) of C57Bl/6 mice. Responses were blocked by the TRPA1 antagonist HC030031 (50 μM; $n = 161$) and by calcium-free external solution ($n = 169$) and were absent in DRG neurons of TRPA1 knock-out mice ($n = 123$; S.E. is displayed as *dashed lines*). MG-sensitive neurons were also mostly activated by AITC (100 μM for 20 s) and occasionally by capsaicin (0.3 μM for 10 s), which stimulated the largest subpopulation (*B*). HC030031 abolished MG-induced calcium transients in a population of neurons that comprised AITC- and/or capsaicin-sensitive cells (*C*; *scale bar*, 100 μm). As shown by the area under the curve, MG-induced responses were concentration-dependent in DRG neurons of C57Bl/6 and TRPV1 knock-out mice, whereas no increase in intracellular calcium was seen in TRPA1 knock-out DRGs (*D*; $n > 60$ each). *E*, concentration-dependent activation of native hTRPA1 and of different mutants involving exchange of cysteine and/or lysine residues. Measurement of calcium signals in transfected HEK 293t cells indicated that MG activated human TRPA1 receptors even at low (3 μM) concentration (*black squares*) with an EC_{50} of 0.7 $\pm$ 0.1 mM. All cells responding to MG also showed an increase in intracellular calcium upon stimulation with carvacrol (250 μM for 30 s), which served as an index for sufficient transfection. In HEK 293t cells transfected with the human TRPA1 C621S/C641S/C665S mutant (hTRPA1–3C; *yellow squares*), the EC_{50} was shifted to higher concentrations ($EC_{50} = 1.8 \pm 0.1$ mM). Single mutation of the lysine residue at position 710 to glutamine (hTRPA1-K710Q; *blue squares*), which cannot be modified by MG, strongly reduced sensitivity to MG application. Residual responsive cells were only found at 3 and 10 mM concentration. The combination of cysteine and lysine mutations hTRPA1–3C/K710Q (*red square*) almost completely abolished responsiveness to MG. Data are mean $\pm$ S.E.

modified by the formation of hemithioacetals (Fig. 3*B* and supplemental Table 1). The appearance of these modifications in different fragments (supplemental Table 1) implies that the three critical Cys residues essential for TRPA1 activation have reacted. Surprisingly, peptide fragments containing disulfide bonds were also detected (Fig. 3*B* and supplemental Table 1). As an example, a comparison of the peak at m/z 3421.42 present in the control with the peak after the treatment with MG (m/z 3419.40) reveals a shift resulting from the loss of two hydrogens (supplemental Fig. 1C). Data analysis revealed the formation of two peptide bonds, each containing one cysteine that was modified with MG. Although proposed to be a possible mechanism for mouse TRPA1 activation (15, 90), disulfide formation of human TRPA1 by natural ligands has not been demonstrated to date but it has recently been shown by structural modeling of mouse TRPA1 binding the synthetic agonist N-methylmaleim-

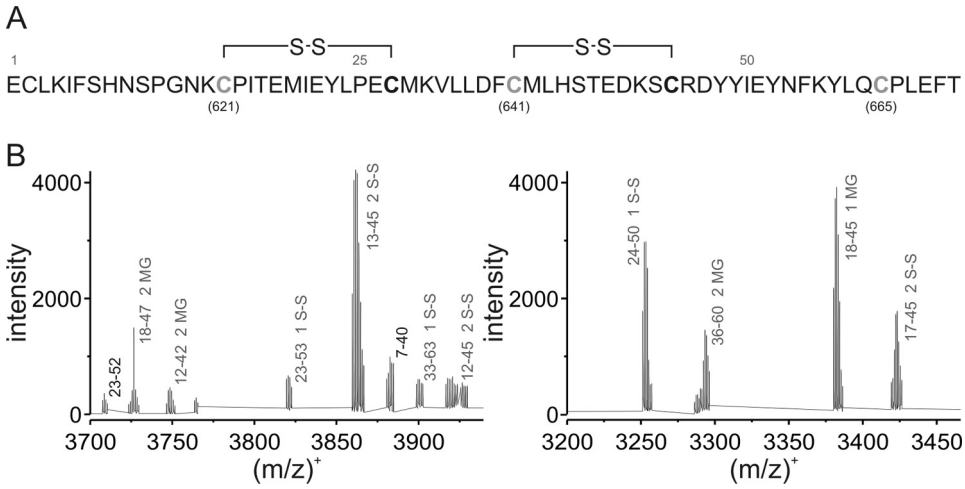

FIGURE 3. **Biochemical characterization of the methylglyoxal-induced modification of critical cysteine residues in hTRPA1.** *A*, amino acid sequence of the model peptide of hTRPA1 (intracellular domain; residues 607–670) containing three cysteine residues essential for receptor activation. *Gray* cysteine residues were found to be covalently modified by MG and subsequently formed disulfide bonds with cysteines in close proximity. *B*, deconvoluted mass spectra of the peptide treated with MG obtained by an ultrahigh resolution ESI-TOF mass spectrometer. Figures represent selected mass ranges with the corresponding peak assignments after treatment with MG for 15 min; fragments originating from the unmodified peptide are labeled in *black*; *gray* labels indicate MG-modified fragments and fragments containing disulfide bonds.

ide (90). Accordingly, formation of disulfide bonds would lead to a conformational change of the whole cytosolic N-terminal domain. We propose that the neighboring cysteine residues could form disulfide bonds with the modified critical cysteines through nucleophilic attack with elimination of hydroxyacetone $CH_2(OH)C(O)CH_3$ (see "Discussion"), which we identified by ESI-TOF mass spectrometry as the main product in a proof-of-concept experiment in which dithiothreitol (DTT) as a model thiol was exposed to MG (supplemental Fig. 1D).

MG-induced Inward Currents and Calcium Transients Can Be Modulated by DTT—Mass spectrometry was performed on a reaction mixture of MG and lysine, and it was confirmed that MG irreversibly binds to lysine (12). The strong reducing agent DTT was unable to resolve this stable adduct (supplemental Fig. 3, A–D). DTT, however, should be able to counteract the hemithioacetal formation of MG with cysteines and the subsequent development of disulfide bonds. Using voltage clamp recordings of hTRPA1 in HEK 293t cells, 3 mM MG-induced inward currents were repeatedly reduced by DTT for the duration of application (Fig. 4*A*). Similar effects were seen in sensory neurons of mice (Fig. 4, *B* and *C*). Although application of DTT 10 min prior to 3 mM MG did not prevent calcium influx in sensory neurons, the responses were significantly shortened (Fig. 4, *B* and *C*). DTT loading also prevented the cross-desensitization of subsequent AITC (100 μM for 20 s) responses, suggesting that sustained covalent modification of TRPA1 cysteines was prevented. Thus, cysteine modifications by MG may also affect the kinetics of the MG responses, *i.e.* slow the deactivation of TRPA1. Interestingly, when DTT was applied to MG-evoked currents of the hTRPA1–3C mutant, this deactivating effect was still present (supplemental Fig. 3E). These data suggest that MG at high concentrations interacts with N-terminal cysteines other than those mutated and that these cysteines also contribute to channel activation and to the kinetic properties of TRPA1 responses.

MG-stimulated CGRP Release from Skin, Sciatic, and Vagus Nerves Is Dependent on TRPA1—As a model to investigate mass activation of peptidergic nerve fibers by MG *in vitro*, stimulated CGRP release was assessed in three different mouse preparations. CGRP release as such signifies neurogenic inflammation, vasodilatation, and plasma extravasation. Axonal CGRP release was studied in desheathed sciatic (Fig. 5, *A* and *B*) and vagus nerves (Fig. 5*C*) upon stimulation with MG because we have recently shown that axonal membranes exhibit vesicular exocytosis of CGRP in a receptor-controlled and calcium-dependent manner (31, 41). Additionally, isolated hairy skin flaps (Fig. 5, *D–F*) were used to investigate CGRP release from peripheral nerve endings. In the sciatic nerve, MG at 1 and 3 mM (both $n = 10$) concentrations significantly stimulated CGRP release (both $p = 0.01$, Wilcoxon), whereas 100 and 300 μM (both $n = 2$) were ineffective (Fig. 5*A*). The vagus nerve showed a dose-dependent response to MG with a threshold concentration of 300 μM (Fig. 5*C*, *inset*). In the hind paw skin, MG at 1 and 3 mM increased CGRP release (both $p = 0.02$, Wilcoxon), whereas 300 μM MG was ineffective (Fig. 5*D*).

For all three preparations, the dependence of MG-induced CGRP release on the activation of TRPA1 receptors was tested using TRPA1 knock-out mice (Fig. 5, *B*, *C*, and *D*), which did not respond to MG at 1 and 3 mM as compared with congenic C57Bl/6 mice (all $p < 0.001$ except for 1 mM in the vagus nerve ($p = 0.05$), *U* tests). In addition, the TRPA1 antagonist HC030031 (50 μM) reduced 1 mM MG-induced CGRP release in both isolated nerve preparations (both $p = 0.01$, Wilcoxon; Fig. 5, *B* and *C*). To exclude a contribution of TRPV1 receptors, which are co-localized with TRPA1 in DRG neurons (13, 42) and even more so in vagal afferents (43, 44), sciatic and vagus nerves from TRPV1 knock-out mice were stimulated with 1 and 3 mM MG; no difference to congenic wild type mice was detected (Fig. 5, *B* and *C*).

To mimic pathophysiological conditions, we investigated whether TRPA1-dependent release of CGRP by MG could be

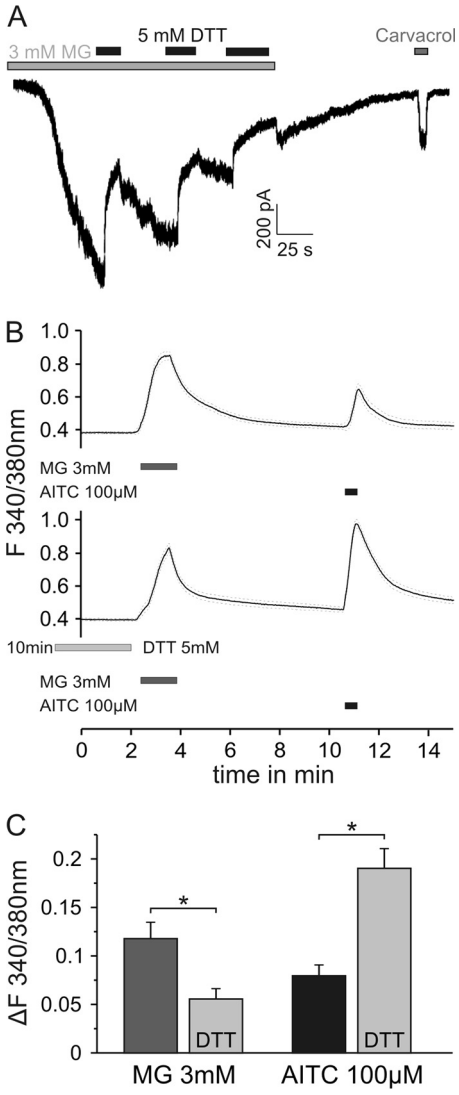

FIGURE 4. **Reducing agents modify MG-induced inward currents in hTRPA1 and calcium transients of DRG neurons.** *A* depicts a representative inward current in HEK 293t cells expressing hTRPA1 induced by MG (3 mM). Co-application of the permanent antioxidant DTT (Cleland's reagent; 5 mM), which impedes modification of cysteine residues and the formation of disulfide bonds, repeatedly deactivated the current. *B*, MG (3 mM) applied for 90 s evoked an increase in intracellular calcium in DRG neurons. DTT at 5 mM applied for 10 min prior to MG shortened the response to MG (*B*, *lower* trace; $p < 0.05$). *C*, DTT loading also prevented the cross-desensitization of the subsequent AITC responses, suggesting a sustained covalent modification of TRPA1 cysteines ($p < 0.001$, both by *t* test of independent samples, $n = 100/145$). Data are mean ± S.E., *, $p < 0.05$.

augmented in the skin by other known endogenous TRPA1 agonists. The unsaturated aldehyde 4-hydroxynonenal (4-HNE), which accumulates under oxidative stress conditions, was tested at 30 and 100 μM (both $n = 8$), but only 100 μM was sufficient to stimulate CGRP release ($p = 0.03$, Wilcoxon; data not shown). The inflammatory mediator and TRPA1 agonist 15deoxy-prostaglandin J_2 concentration-dependently increased CGRP release at 100 and 300 μM (both $p = 0.01$, $n = 8$ and $n = 7$, Wilcoxon, data not shown). When 100 μM 4-HNE was combined with a subliminal MG concentration of 300 μM, the resulting release was markedly enhanced compared with the individual compounds ($p < 0.001$, *U* test; Fig. 5, *E* and *F*). Also the combination of 300 μM 15deoxy-prostaglandin J_2 and 300 μM MG was more effective than the individual compounds ($p < 0.001$ and $p = 0.02$, *U* test; Fig. 5*F*).

Inflammatory mediators like bradykinin and prostaglandin can functionally sensitize TRPA1 by activation of phospholipase C (PLC) and protein kinase A (PKA) (38, 45). Therefore, we used 10 μM forskolin to activate PKA, which alone did not augment cutaneous CGRP release but sensitized the subliminal effect of 300 μM MG ($p < 0.0001$, *U* test; Fig. 5*F*). The same applied to 100 μM 2,4,6-trimethyl-*N*-[3-(trifluoromethyl)phenyl]benzenesulfonamide, which is known to activate PLC and sensitize TRPA1 ($p = 0.01$, *U* test). Co-application of forskolin and 2,4,6-trimethyl-*N*-[3-(trifluoromethyl)phenyl]benzenesulfonamide did not further enhance CGRP release. Together, the CGRP release experiments demonstrated selective activation of TRPA1-expressing termini and nerve fibers by acutely applied MG and a marked facilitation of MG by co-activators and second messenger pathways.

MG-induced axonal CGRP release indicated the functional expression of TRPA1 along peripheral nerve C-fibers, mediating an excitatory response. However, CGRP measurements cover the peptidergic subpopulation of nociceptors but not the IB4-binding subpopulation or non-nociceptive A-fibers. To include them, the compound action potential of sciatic nerves was adapted to *in vitro* experimentation.

MG Reduces Conduction Velocity and Amplitude of the Sciatic Nerve Compound Action Potential in Wild Type but Not TRPA1 Knock-out Mice—Recording the electrically evoked CAP from isolated sciatic nerve in a three-compartment dish (34) and taking the decrease of amplitude as an index of activation by concomitant (chemical) stimulation (46), the CAP of the fast conducting myelinated fibers was not altered in any respect by superfusing the nerve for 20 min with 10 mM MG (data not shown). However, the C-fiber CAP (Fig. 6*A*) showed a progressive slowing of the conduction velocity with recovery during washout of MG, that can be interpreted as a discharge activity-dependent slowing, that is typical for chemosensitive C-fibers (47, 48). The amplitude of the C-fiber CAP instantly decreased with the onset of MG superfusion and then progressively declined further. The latter MG response phase most likely reflects desynchronization among fibers of the electrically evoked action potentials due to differential activity-dependent slowing (47). However, the sudden drop of the CAP amplitude at the onset of MG does not correspond to the progressive slowing and may reflect an additional impairment by MG of voltage-gated sodium channel functions, leading to a block or reduction of the CAP amplitude (49). Essentially, however, both MG effects (slowing and amplitude reduction) appear to be secondary to activation of TRPA1 because sciatic nerves from the knock-out mice showed neither alteration (Fig. 6, *B* and *C*; $p < 0.05$ and $p < 0.01$, respectively; $n = 6$; *U* test). Perhaps MG through TRPA1 activation causes sustained depolarization and inactivation of voltage-gated sodium channels in the background of asynchronous ongoing discharge in C-fibers.

MG Differentially Activates Subtypes of Cutaneous Afferents in Vitro—To evaluate the effects of MG on subtypes of nociceptors and one representative myelinated low threshold mechanoreceptor, we used the skin saphenous nerve preparation to record action potential discharge from cutaneous single C- and

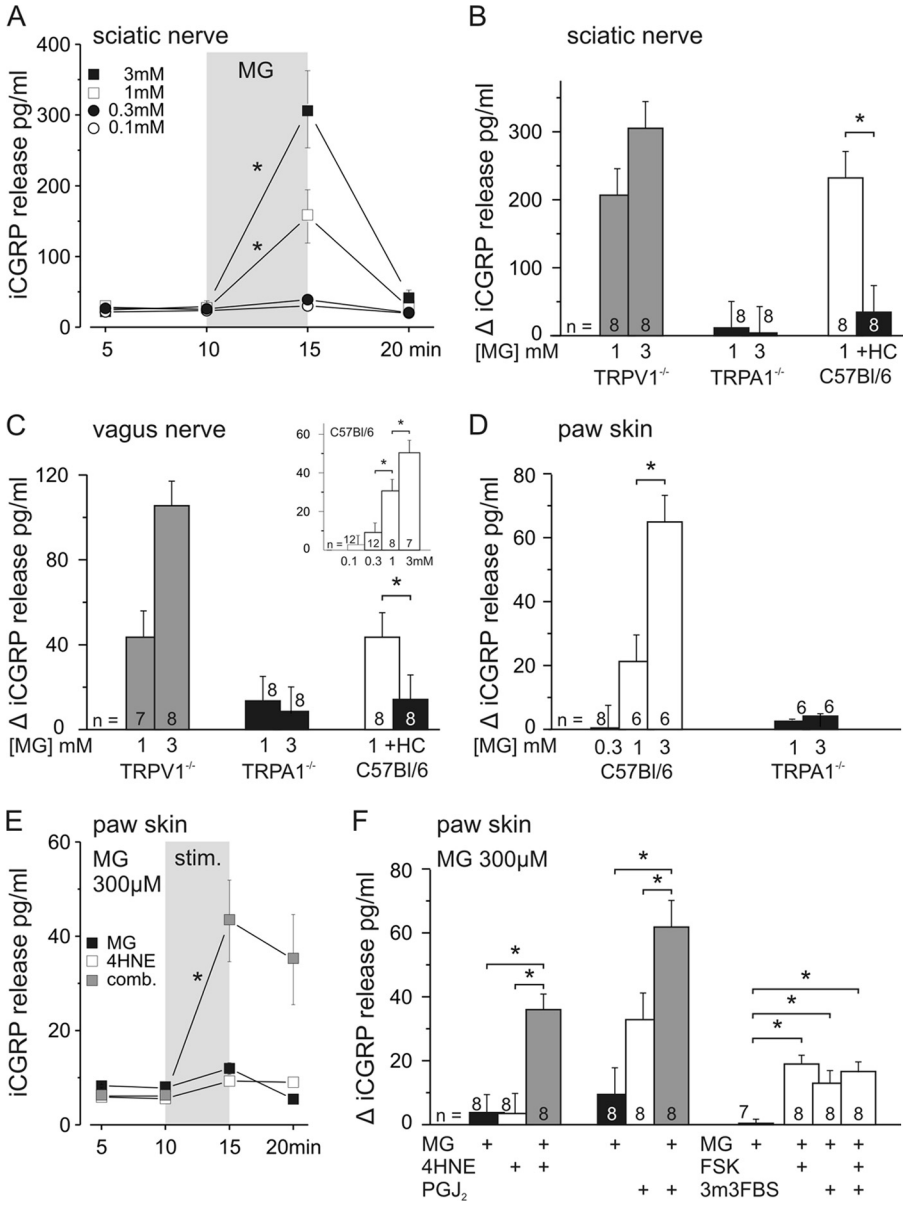

FIGURE 5. **MG-stimulated CGRP release from sciatic and vagus nerves is dependent on TRPA1 receptors.** The effects of MG on CGRP release from isolated sciatic nerves, vagus nerves, and paw skin of C57Bl/6 mice are shown. MG concentration-dependently stimulated CGRP release from desheathed sciatic nerve (*A* and *B*) and vagus nerve (*C* and *inset*). CGRP release was stimulated by 300 μM (vagus nerve only), 1 mM, and 3 mM MG. MG stimulated nearly the same amount of CGRP release from sciatic and vagus nerves of TRPV1 knock-out mice; the response was absent in TRPA1 knock-out mice and was abolished by TRPA1 antagonist HC030031 (*HC*) at 50 μM. *D*, MG-stimulated CGRP release from paw skin was concentration-dependent in C57Bl/6 mice and absent in congenic TRPA1 knock-out mice. *E*, MG at 300 μM was not sufficient to stimulate CGRP release alone but in combination (*comb.*) with an inefficient concentration of 4-HNE (100 μM) significantly stimulated (*stim.*) CGRP release from paw skin. *F*, MG effects were augmented by combination with other endogenous TRPA1 agonists as shown for 4-HNE (100 μM) and 15deoxy-prostaglandin J_2 (PGJ_2) (300 μM). Sensitizing TRPA1 receptors by co-activation of the adenylyl cyclase/protein kinase A pathway (forskolin (*FSK*) at 10 μM), phospholipase C (2,4,6-trimethyl-*N*-[3-(trifluoromethyl)phenyl]benzenesulfonamide (*3m3FBS*) at 100 μM), or both yielded significant increases in CGRP release upon 300 μM MG. Data are mean ± S.E., *, $p < 0.05$. *iCGRP*, CGRP concentrations as measured by CGRP EIA.

Aδ-fibers ($n = 47$) of C57Bl/6 and TRPA1 knock-out mice. The sensory properties of the fibers and responses to MG application are listed in supplemental Table 2. Each fiber underwent the same experimental protocol (Fig. 7): conduction velocity, von Frey threshold, noxious cold and heat stimulation; thereafter, the receptive field was isolated with a metal ring and superfused with 10 mM MG for at least 10 min while cold and heat sensitivity were retested.

MG at 1 mM concentration did not induce any action potential discharge in C-fibers within 30 min of superfusion. However, 10 mM activated about 85% of the C-nociceptors and one distinct subpopulation of Aδ-fibers. The sensitivity to 10 mM MG varied. As in wild type mice, C-mechano-, heat-, and cold-sensitive (C-MHC) fibers were frequently more responsive than C-MH fibers (one-way analysis of variance, $F(1,18) = 11.0$, $p < 0.01$; Fig. 7, *A* and *B*). C-MHC fibers also exhibited stronger initial and sustained responses to MG that often persisted with irregular ongoing discharge throughout the application period (Fig. 7*D*). The biphasic, dynamic-static response pattern indicates that two different mechanisms are involved: first, activation of TRPA1 that desensitizes in 2–3 min and second, an excitatory mechanism of yet unknown origin. This interpreta-

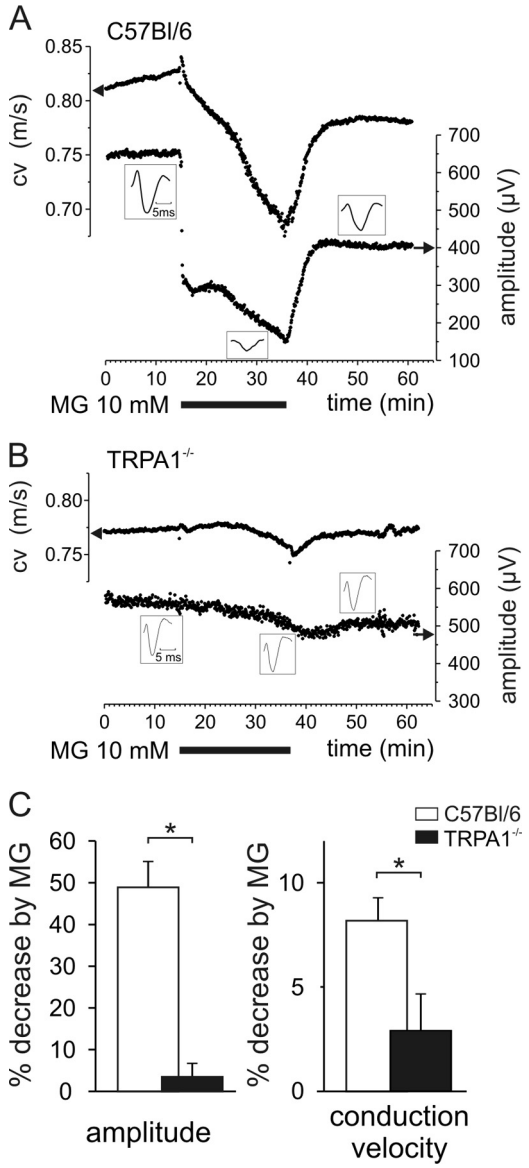

FIGURE 6. **MG reduces conduction velocity and amplitude of the sciatic nerve compound action potential in wild type but not TRPA1 knock-out mice.** *A*, MG at 10 mM for 20 min reduced conduction velocity (*cv*) progressively, whereas the amplitude decreased instantaneously and then declined further. Upon washout, both effects recovered rapidly and largely. *B*, no effects of MG in TRPA1 knock-out mice. *C*, MG decreased conduction velocity and amplitude in wild type mice measured after 15-min superfusion but not in TRPA1 knock-out mice. Data are mean ± S.E., *, $p < 0.05$.

tion is derived from the recordings from TRPA1 knock-out mice (Fig. 7*E*) that lacked the dynamic response at the onset of MG superfusion but showed sustained ongoing discharge; at least the C-MHC fibers did so, whereas the mechano- and heat-sensitive units hardly responded at all. The number of action potentials elicited in the first 3 min of MG superfusion was significantly reduced in the C-MHC fibers as well as in the C-MH fibers recorded in TRPA1 knock-out mice compared with control mice ($p = 0.02$ and $p = 0.002$, *U* test).

In total, 15 Aδ-fibers were tested with MG. Three high threshold mechanoreceptive Aδ-fibers did not respond, and the other 12 Aδ-units formed a homogenous subgroup defined by von Frey thresholds below 1 mN and rapid adaptation (down hair receptors), four of which exhibited the most vigorous responses to MG application. The representative example in Fig. 6*D* shows such a strong, slowly adapting response to MG. This initially cold-insensitive fiber was clearly sensitized to cold stimulation during MG superfusion.

Heat responsiveness of C-MH and C-MHC fibers in C57Bl/6 mice was not changed during and after MG application (supplemental Table 2). However, the data indicate a possibly increased sensitivity to cold stimulation after MG treatment of the receptive field. C-MHC fibers were activated at higher temperatures (supplemental Table 2) and showed an increased mean cold response after MG of 15 ± 3 spikes/stimulus compared with 9 ± 3 spikes/stimulus before), but both parameters were not significantly different. The C-MHC fiber shown in Fig. 7*B* had only a sparse initial cold response but was sensitized to cold stimulation during MG superfusion. Such cold sensitization was observed in four of nine C-MHC fibers; these fibers exhibited an elevation of their cold threshold by more than 5 °C. In addition, three of 11 C-MH fibers developed *de novo* cold responsiveness after MG application and then showed a mean cold threshold of 22.4 ± 3 °C and a mean cold response of 15 ± 7.4 spikes/stimulus, which is similar to the cold responsiveness of C-MHC fibers (15 ± 3 spikes/stimulus). These conspicuous findings on cold sensitivity may provide at least some circumstantial evidence for MG-induced hypersensitivity of skin nerve termini to cooling that would correspond to the established role of TRPA1 in various animal models of cold hyperalgesia (50).

DISCUSSION

MG activated TRPA1 receptor channels in DRG neurons and transfected HEK 293t cells by modification of intracellular N-terminal lysine and cysteine residues. MG-stimulated CGRP release from peptidergic nerves was dependent on TRPA1 but not TRPV1 receptors and could be sensitized by the endogenous TRPA1 agonist 4-HNE and by activation of the PKA/PLC pathways. Finally, MG led to activity-dependent slowing of C-fiber conduction in peripheral nerves and activated Aδ- and C-nociceptors *in vitro* which at least in part involved TRPA1.

MG is mainly derived from triose phosphates of glycolysis (2) and can be measured in plasma of healthy subjects at concentrations of 200–500 nM (6). A minor source of MG is acetone from ketone bodies (51) and aminoacetone metabolism (52), which indicates enhanced production upon lipid peroxidation as well as upon excessive lipid and protein catabolism. Exceeding 800–900 nM in pathological conditions, MG plasma levels are strongly dependent on renal function as they have been shown to be negatively correlated with creatinine clearance (53) and therefore to increase in a stage-dependent manner with chronic renal failure independently of concomitant diabetes (6). MG in plasma reflects the degree of hyperglycemia (54) in diabetic patients due to enhanced production and impaired enzymatic degradation by glyoxalase I (3). Neurons take up glucose independently of insulin and more so under the condition of hyperglycemia. In addition, glyoxalase I expression and activity are constitutively very low in the peripheral nervous system (49) consistent with previous findings that MG concentrations are high in sciatic nerve tissue compared with other organs such as the liver and further elevated in diabetic rats (55). Thus, MG

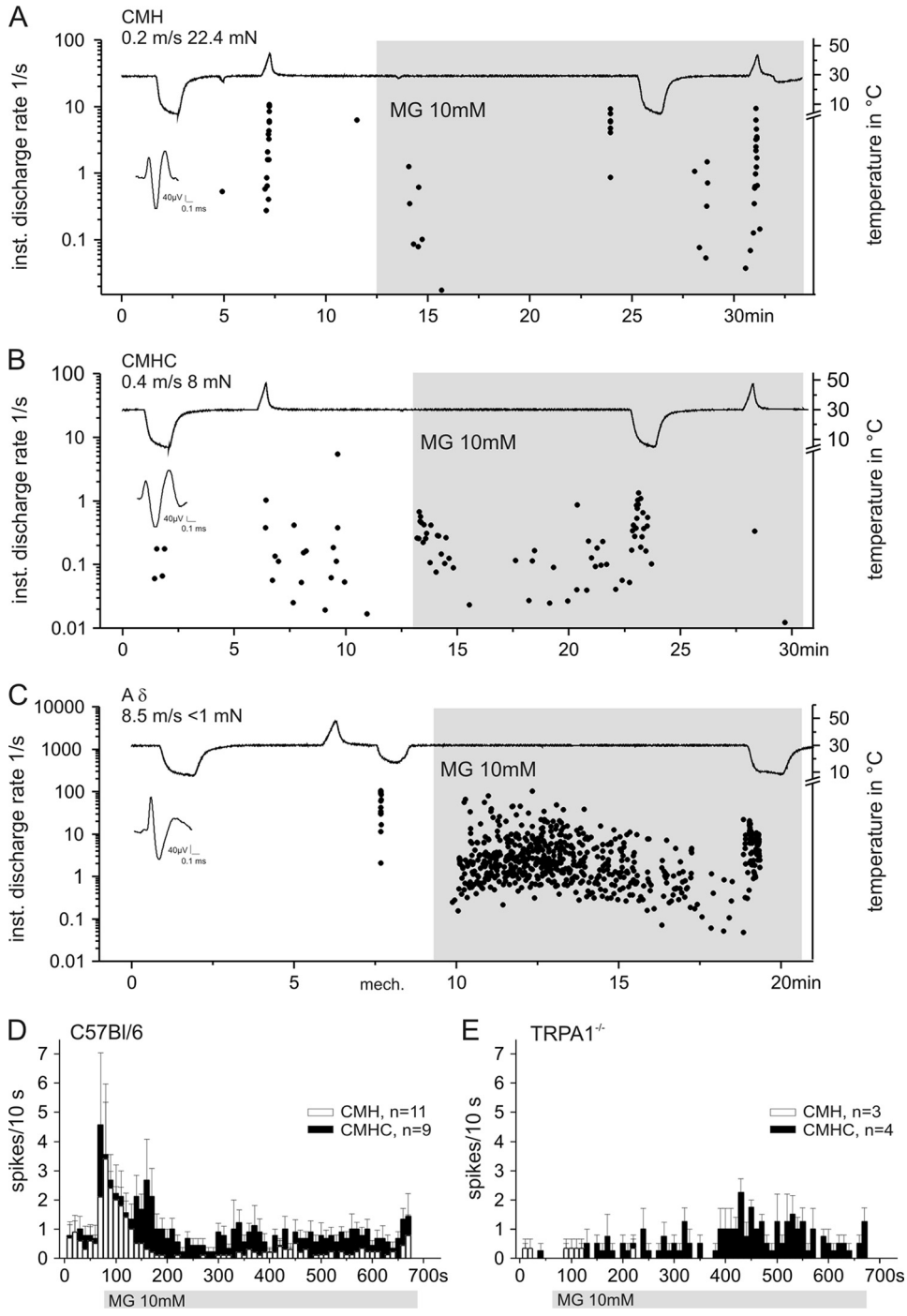

FIGURE 7. **MG differentially activates different types of cutaneous nociceptors *in vitro*.** *A* and *B*, recordings from two C-fibers using the skin saphenous nerve preparation of the mouse. MG (10 mM) was applied to the isolated receptive fields for about 20 min and caused a stronger and long lasting excitation of C-MHC fibers (*B*). The fiber shown in *B* exhibited a clearly increased response to cold stimulation during MG application. *C* depicts the strong excitatory effect of MG on a subgroup of low threshold mechanosensitive (*mech.*) A-fibers. The representative recording shows an Aδ-fiber that was activated by MG and sensitized to cold stimulation applied during MG application. *D* and *E*, average MG response histograms (spikes/10 s) of C-MHC fibers (*closed bars*) and C-MH fibers (*open bars*) in wild type (*D*) and TRPA1 knock-out mice (*E*). Obviously, the initial phasic response was lost. *inst.*, instantaneous; *mN*, millinewtons. Data are mean ± S.E.

concentrations are much higher intra- than extracellularly, in particular in neurons; in addition, (reversible) binding to cell proteins likely traps MG intracellularly (1, 56). In fact, the intracellular MG concentration in naïve mouse DRG neurons (1.5 μM) was much higher than the plasma levels (2). Concentrations higher than pathological plasma concentrations were thus required to activate sensory neurons in culture or in isolated preparations, although TRPA1-overexpressing HEK 293t cells responded to a concentration as low as 1 μM MG with a calcium influx that reached the same magnitude as with 3 mM MG as a stimulus. MG is hydrophilic and in aqueous solution fully hydrated, forming diols and tetrols (57, 58). MG readily passes through neuronal plasma membranes (56). Hence, the intracellular generation and pathological accumulation of MG could be

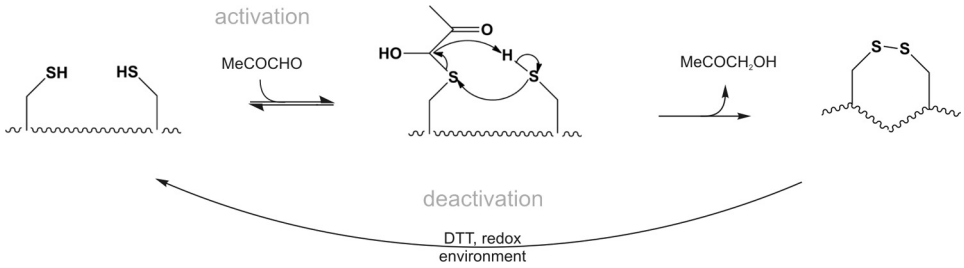

FIGURE 8. **Proposed reaction mechanism for methylglyoxal-induced modification of cysteine residues of TRPA1.** MG (MeCOCHO) reversibly reacts with one of the cysteine residues of the N-terminal intracellular part of TRPA1 to form hemithioacetals. This probably leads to conformational changes sufficient to activate the channel. The hemithioacetal increases the reactivity of the sulfur, facilitating disulfide bond formation with an SH-cysteine residue in close proximity. The reductive intracellular environment or DTT (see supplemental Fig. 2) restores the original state of TRPA1 and deactivates it.

mimicked by extracellular short term application (*e.g.* 90 s), which achieved a rise from 1.5 to 2.2 μM in DRG neurons.

It is widely accepted that lysine and arginine are primary targets for the glycation reaction with MG. Although they form an irreversible, stable adduct, the cysteine modification is reversible. Our calcium imaging studies on various hTRPA1 mutants indicate that the importance of lysine at position 710 for activation of TRPA1 increases at high MG concentrations, leading to faster channel activation and an earlier rise of intracellular calcium (supplemental Fig. 1B). However, it is remarkable that none of the five lysines in the model peptide (607–670) of N-terminal hTRPA1 were modified (Fig. 3*A*). Lysine (or arginine) 710 might have an exceptional affinity for MG, making it a cooperative binding site for TRPA1 activation. Besides possible differences in accessibility of amino acids in the native TRPA1 channel, it also has to be taken into account that MG reacts several orders of magnitude faster with cysteine than with any other amino acid (rate constant for cysteine, 4.1×10^4 M^{-1} s^{-1}, compared with 8.5×10^{-3} M^{-1} s^{-1} for arginine and 6.8×10^{-3} M^{-1} s^{-1} for lysine; Ref. 12). The binding of MG to cysteine is reversible and leads to hemithioacetal and subsequent formation of disulfide bonds (Fig. 8), which would likely result in a conformational change of the entire cytosolic domain. Formation of disulfide bonds in the N terminus by a synthetic cysteine modifying agent of mouse TRPA1 has recently been demonstrated on a structural level (90). Indicated by a rightward shift in the concentration-response curve of the human triple cysteine mutant in calcium imaging and patch clamp studies using DTT, these cysteine modifications likely affect the activation as well as kinetics of channel opening and deactivation. Depending on the position and number of the critical cysteines modified, the number and location of the disulfide bonds will vary. As deduced from reports that TRPA1 is also activated by iodoacetamide, which alkylates cysteines but prevents disulfide bond formation (26), it can be assumed that disulfide bond formation is secondary to channel gating likely due to the prior step of hemithioacetal formation. Only the cysteines have been reported to be essential for mouse TRPA1 activation by direct modification, and lysine-modifying agents were without any effect (26). However, the strong reducing agent DTT, which interferes with cysteine modification, could not prevent activation of mouse sensory neurons by MG but only shortened the MG-evoked calcium responses (Fig. 4, *B* and *C*). On the other hand, human TRPA1 (in HEK 293t cells) was clearly deactivated by DTT, which can prevent hemithioacetal formation and resolve disulfide bonds between cysteines. Thus, sustained TRPA1 activation by MG through cysteine modifications remains a valid working hypothesis for both mouse and human TRPA1. MG-induced inward currents in the C621S/C641S/C665S hTRPA1–3C mutant could be influenced by DTT, indicating that further cysteines might contribute to modification of TRPA1 and responsiveness to MG at higher concentrations.

Glycation and oxidative stress have been reported to be responsible for MG-induced neurotoxicity (59–61). MG as well as glyoxal mediate rapid non-enzymatic glycation of proteins and other substrates, promoting the formation of advanced glycation end products, which have been found to foster the formation of reactive oxygen species; therefore, MG is generally associated with high oxidative stress (3). Several metabolic products of oxidative stress have been shown to activate TRPA1 such as H_2O_2, 4-HNE (44), and 15deoxy-prostaglandin J_2 (18). Thus, MG accumulation coincides with elevated levels of other endogenous TRPA1 agonists, and it is also involved in the formation of reactive oxygen species. We demonstrated cooperative effects of endogenous TRPA1 agonists in MG-stimulated CGRP release from nerve endings. PKA and PLC have been shown to be involved in sensitization of TRPA1 (*e.g.* by bradykinin), a mechanism that could account for sensitization under inflammatory conditions (19). In the presence of PKA and PLC activators, CGRP release could be stimulated with concentrations of MG that were below threshold in otherwise untreated paw skin preparations. Enhanced trafficking of TRPA1 to the cell membrane has been described as a mechanism of sensitization by PKA and PLC (45). A mediator capable of PLC activation is endothelin (62), which also accounts for cardiovascular complications accompanying diabetes (63) and chronic renal failure (64). Endothelin receptors are expressed in sensory neurons (65), and the endothelin 1 receptor has been described to be involved in pain signaling as well as sensitizing human C-nociceptors (66).

Recently, TRPA1 receptors were suggested to be involved in mechanical hypersensitivity of nociceptors in a diabetes model (23, 24); diabetes-induced formation of endogenous compounds like 4-HNE (67, 68) was proposed to contribute. Increased sensitivity and excitability of peripheral nociceptors in painful diabetic neuropathy were attributed to altered expression and functional properties of ion channels and membrane receptors such as TRPV1 (69, 70), T-type calcium channels (71, 72), and diverse voltage-gated sodium channels (73,

74). In our models, involvement of TRPV1 receptors in membrane currents, MG-induced Ca^{2+} influx, and CGRP release could be excluded as MG did not activate cells transfected with TRPV1 even at high concentrations, and effects in preparations of TRPV1 knock-out animals were undistinguishable from those observed in wild type animals. However, about 90% of the C-fibers recorded from the skin nerve preparation expressing TRPA1 receptors (42) were directly activated by MG superfusion in wild type mice. C-fibers recorded from TRPA1 knock-out mice still responded to MG application (Fig. 7*F*), but the initial dynamic response was completely absent. If TRPA1 was deleted, only a delayed tonic activation was retained to which a second activation mechanism, perhaps a modification of sodium channels, may contribute. Furthermore, MG caused a fast and robust activity-dependent slowing of C-fiber conduction (Fig. 6) that was absent in peripheral nerves of TRPA1 knock-out mice. Such axons, at least the peptidergic axons, are well equipped with functional TRPA1 channels (31). Activation by MG and resulting depolarization likely foster the proposed biophysical mechanism of activity-dependent slowing, which is a reduction of sodium channel availability by inactivation (48). Together, these data substantiate the contribution of TRPA1 receptors to MG-induced excitation of primary sensory neurons. Other effects of MG leading to increased excitability are not ruled out and have been described earlier. For example, 300 μM MG induced a slowly developing depolarization in cortical neurons (75), whereas a fast depolarization was observed by 1 mM MG in isolated rat pancreatic islet cells (76). However, in human skin, MG is plainly a noxious and irritant compound; intradermal injections caused burning pain for a few minutes and a typical axon reflex flare response indicative of peptidergic nociceptor activation (10 mM; 15 μl).[3]

In addition, results from the C-fiber recordings suggest an increase of cold sensitivity after MG superfusion of the receptive field. We observed increased responsiveness both of originally cold-sensitive fibers, which increased their responses to cold, and of cold-insensitive fibers, which showed *de novo* responsiveness. Cold sensitivity mediated by TRPA1 receptors has been shown in different models, and its contribution to cold hypersensitivity under neuropathic and inflammatory conditions has become a consensus (77, 78). Other cold-sensitive transduction channels like TRPM8 may contribute to painful cold sensations because naïve cold responsiveness was normal in C-fibers recorded from TRPA1 knock-out mice in an experimental approach similar to ours (79). Painful diabetic neuropathy is accompanied by deteriorated cold perception (80), and these patients suffer from impaired thermoregulation (81). Although unpleasant cold feet sensations are common in diabetic patients, painful cold sensations have not been reported. Streptozotocin-induced diabetic animals develop behavioral cold allodynia or hyperalgesia (82, 83). Unfortunately, nothing is known about the cold responsiveness of C-fibers in diabetic wild type *versus* TRPA1 knock-out mice or a possible contribution of TRPA1 to the cold feet sensations of diabetics, which were beyond the scope of this study.

[3] P. Reeh and M. Eberhardt, unpublished observation.

Aδ-fibers with low mechanical thresholds are not considered to express functional TRPA1 receptors (42, 79, 84). Consequently, most of the recorded Aδ-fibers (11 of 15) did not respond to MG application. The remaining four rapidly adapting Aδ-fibers (<1 mN were vigorously excited upon MG application (Fig. 7*C*). Fibers with similar mechanical responsiveness and conduction velocity have been classified as down hair receptors (85, 86). T-type calcium channels among DRG neurons are almost exclusively expressed in these down hair receptors and reported to control excitability and mechanosensory transduction (85, 87). Interestingly, T-type calcium channels are up-regulated in medium size rat DRG neurons and show increased excitability in diabetic rats (71, 72). Whether post-translational modification of T-type calcium channels by MG (for 10 min) contributes to the massive MG responses of some Aδ-fibers remains to be investigated. Sensitized Aδ- and Aβ-fibers that exhibit burstlike discharge and lowered mechanical thresholds in streptozotocin-induced diabetic rats have been proposed to contribute to the development of tactile allodynia in painful diabetic neuropathy (88). Whether TRPA1 like TRPV1 is up-regulated in diabetic neuropathy is unknown, but in a partial nerve injury model, mechano- as well as cold sensitivity of Aδ-fibers was increased (84). In addition, the particular MG sensitivity of some Aδ-fibers could also be explained by a lack of glyoxalase I in these fibers and a resulting inability to detoxify MG. In fact, it is interesting that the expression of glyoxalase I has recently been reported to be restricted to small unmyelinated peptidergic neurons excluding Aδ-units (89).

Distinct cysteine residues and for human TRPA1 one lysine in the N terminus of nociceptive TRPA1 receptor channels are required for activation by electrophilic compounds like MG (25, 26). Here, we show that MG activates inward currents and calcium influx in transfected cells and sensory neurons, slows conduction velocity in unmyelinated peripheral nerve fibers, and stimulates release of proinflammatory neuropeptides and action potential firing in cutaneous nociceptors. We propose a new mechanism of intramolecular disulfide bond formation by MG-induced hemithioacetal as the intermediate. This chemical reaction seems to sustain the activation of TRPA1.

MG as a reactive cytotoxic metabolite is increased in different pathophysiological conditions like uremia and diabetes; activates TRPA1, the polymodal chemosensor of the nociceptive neuron; and cooperates with other noxious metabolites. By these actions, MG may contribute to neuropathic sequelae accompanying those diseases that affect an increasing number of people in our aging population. Therefore, blockade of TRPA1, reduction of MG formation, or scavenging may emerge as therapeutic options in these conditions.

Acknowledgments—We thank S. E. Jordt for providing TRPA1 vectors and B. Turnquist for supplying customized DAPSYS versions. We thank I. Izydorczyk, A. Kuhn, and S. Haux-Oertel for excellent technical assistance.

REFERENCES

1. Thornalley, P. J. (1996) Pharmacology of methylglyoxal: formation, modification of proteins and nucleic acids, and enzymatic detoxification—a role in pathogenesis and antiproliferative chemotherapy. *Gen. Pharmacol.*

27, 565–573
2. Thornalley, P. J., Langborg, A., and Minhas, H. S. (1999) Formation of glyoxal, methylglyoxal and 3-deoxyglucosone in the glycation of proteins by glucose. *Biochem. J.* **344,** 109–116
3. Brownlee, M. (2001) Biochemistry and molecular cell biology of diabetic complications. *Nature* **414,** 813–820
4. Thornalley, P. J. (1990) The glyoxalase system: new developments towards functional characterization of a metabolic pathway fundamental to biological life. *Biochem. J.* **269,** 1–11
5. Han, Y., Randell, E., Vasdev, S., Gill, V., Gadag, V., Newhook, L. A., Grant, M., and Hagerty, D. (2007) Plasma methylglyoxal and glyoxal are elevated and related to early membrane alteration in young, complication-free patients with type 1 diabetes. *Mol. Cell. Biochem.* **305,** 123–131
6. Nakayama, K., Nakayama, M., Iwabuchi, M., Terawaki, H., Sato, T., Kohno, M., and Ito, S. (2008) Plasma α-oxoaldehyde levels in diabetic and nondiabetic chronic kidney disease patients. *Am. J. Nephrol.* **28,** 871–878
7. Suzuki, Y., Sato, J., Kawanishi, M., and Mizumura, K. (2002) Tissue glucose level modulates the mechanical responses of cutaneous nociceptors in streptozotocin-diabetic rats but not normal rats *in vitro*. *Pain* **99,** 475–484
8. Suzuki, Y., Sato, J., Kawanishi, M., and Mizumura, K. (2002) Lowered response threshold and increased responsiveness to mechanical stimulation of cutaneous nociceptive fibers in streptozotocin-diabetic rat skin *in vitro*—correlates of mechanical allodynia and hyperalgesia observed in the early stage of diabetes. *Neurosci. Res.* **43,** 171–178
9. Fuchs, D., Birklein, F., Reeh, P. W., and Sauer, S. K. (2010) Sensitized peripheral nociception in experimental diabetes of the rat. *Pain* **151,** 496–505
10. Lapolla, A., Fedele, D., Reitano, R., Bonfante, L., Pastori, G., Seraglia, R., Tubaro, M., and Traldi, P. (2005) Advanced glycation end products/peptides: an *in vivo* investigation. *Ann. N.Y. Acad. Sci.* **1043,** 267–275
11. Miyata, T., van Ypersele de Strihou, C., Kurokawa, K., and Baynes, J. W. (1999) Alterations in nonenzymatic biochemistry in uremia: origin and significance of "carbonyl stress" in long-term uremic complications. *Kidney Int.* **55,** 389–399
12. Lo, T. W., Westwood, M. E., McLellan, A. C., Selwood, T., and Thornalley, P. J. (1994) Binding and modification of proteins by methylglyoxal under physiological conditions. A kinetic and mechanistic study with *N*α-acetylarginine, *N*α-acetylcysteine, and *N*α-acetyllysine, and bovine serum albumin. *J. Biol. Chem.* **269,** 32299–32305
13. Story, G. M., Peier, A. M., Reeve, A. J., Eid, S. R., Mosbacher, J., Hricik, T. R., Earley, T. J., Hergarden, A. C., Andersson, D. A., Hwang, S. W., McIntyre, P., Jegla, T., Bevan, S., and Patapoutian, A. (2003) ANKTM1, a TRP-like channel expressed in nociceptive neurons, is activated by cold temperatures. *Cell* **112,** 819–829
14. Jordt, S. E., Bautista, D. M., Chuang, H. H., McKemy, D. D., Zygmunt, P. M., Högestätt, E. D., Meng, I. D., and Julius, D. (2004) Mustard oils and cannabinoids excite sensory nerve fibres through the TRP channel ANKTM1. *Nature* **427,** 260–265
15. Takahashi, N., Kuwaki, T., Kiyonaka, S., Numata, T., Kozai, D., Mizuno, Y., Yamamoto, S., Naito, S., Knevels, E., Carmeliet, P., Oga, T., Kaneko, S., Suga, S., Nokami, T., Yoshida, J., and Mori, Y. (2011) TRPA1 underlies a sensing mechanism for O_2. *Nat. Chem. Biol.* **7,** 701–711
16. Wang, Y. Y., Chang, R. B., and Liman, E. R. (2010) TRPA1 is a component of the nociceptive response to CO_2. *J. Neurosci.* **30,** 12958–12963
17. Wang, Y. Y., Chang, R. B., Allgood, S. D., Silver, W. L., and Liman, E. R. (2011) A TRPA1-dependent mechanism for the pungent sensation of weak acids. *J. Gen. Physiol.* **137,** 493–505
18. Andersson, D. A., Gentry, C., Moss, S., and Bevan, S. (2008) Transient receptor potential A1 is a sensory receptor for multiple products of oxidative stress. *J. Neurosci.* **28,** 2485–2494
19. Wang, S., Dai, Y., Fukuoka, T., Yamanaka, H., Kobayashi, K., Obata, K., Cui, X., Tominaga, M., and Noguchi, K. (2008) Phospholipase C and protein kinase A mediate bradykinin sensitization of TRPA1: a molecular mechanism of inflammatory pain. *Brain* **131,** 1241–1251
20. Bandell, M., Story, G. M., Hwang, S. W., Viswanath, V., Eid, S. R., Petrus, M. J., Earley, T. J., and Patapoutian, A. (2004) Noxious cold ion channel TRPA1 is activated by pungent compounds and bradykinin. *Neuron* **41,** 849–857
21. Belvisi, M. G., Dubuis, E., and Birrell, M. A. (2011) Transient receptor potential A1 channels: insights into cough and airway inflammatory disease. *Chest* **140,** 1040–1047
22. Engel, M. A., Leffler, A., Niedermirtl, F., Babes, A., Zimmermann, K., Filipović, M. R., Izydorczyk, I., Eberhardt, M., Kichko, T. I., Mueller-Tribbensee, S. M., Khalil, M., Siklosi, N., Nau, C., Ivanović-Burmazović, I., Neuhuber, W. L., Becker, C., Neurath, M. F., and Reeh, P. W. (2011) TRPA1 and substance P mediate colitis in mice. *Gastroenterology* **141,** 1346–1358
23. Wei, H., Koivisto, A., Saarnilehto, M., Chapman, H., Kuokkanen, K., Hao, B., Huang, J. L., Wang, Y. X., and Pertovaara, A. (2011) Spinal transient receptor potential ankyrin 1 channel contributes to central pain hypersensitivity in various pathophysiological conditions in the rat. *Pain* **152,** 582–591
24. Wei, H., Koivisto, A., and Pertovaara, A. (2010) Spinal TRPA1 ion channels contribute to cutaneous neurogenic inflammation in the rat. *Neurosci. Lett.* **479,** 253–256
25. Hinman, A., Chuang, H. H., Bautista, D. M., and Julius, D. (2006) TRP channel activation by reversible covalent modification. *Proc. Natl. Acad. Sci. U.S.A.* **103,** 19564–19568
26. Macpherson, L. J., Dubin, A. E., Evans, M. J., Marr, F., Schultz, P. G., Cravatt, B. F., and Patapoutian, A. (2007) Noxious compounds activate TRPA1 ion channels through covalent modification of cysteines. *Nature* **445,** 541–545
27. Cvetkov, T. L., Huynh, K. W., Cohen, M. R., and Moiseenkova-Bell, V. Y. (2011) Molecular architecture and subunit organization of TRPA1 ion channel revealed by electron microscopy. *J. Biol. Chem.* **286,** 38168–38176
28. Babes, A., Fischer, M. J., Reid, G., Sauer, S. K., Zimmermann, K., and Reeh, P. W. (2010) Electrophysiological and neurochemical techniques to investigate sensory neurons in analgesia research. *Methods Mol. Biol.* **617,** 237–259
29. Liu, H., and Naismith, J. H. (2008) An efficient one-step site-directed deletion, insertion, single and multiple-site plasmid mutagenesis protocol. *BMC Biotechnol.* **8,** 91
30. Chaplen, F. W., Fahl, W. E., and Cameron, D. C. (1996) Method for determination of free intracellular and extracellular methylglyoxal in animal cells grown in culture. *Anal. Biochem.* **238,** 171–178
31. Weller, K., Reeh, P. W., and Sauer, S. K. (2011) TRPV1, TRPA1, and CB1 in the isolated vagus nerve—axonal chemosensitivity and control of neuropeptide release. *Neuropeptides.* **45,** 391–400
32. Sauer, S. K., Bove, G. M., Averbeck, B., and Reeh, P. W. (1999) Rat peripheral nerve components release calcitonin gene-related peptide and prostaglandin E2 in response to noxious stimuli: evidence that nervi nervorum are nociceptors. *Neuroscience* **92,** 319–325
33. Bretag, A. H. (1969) Synthetic interstitial fluid for isolated mammalian tissue. *Life Sci.* **8,** 319–329
34. Bremer, M., Fröb, F., Kichko, T., Reeh, P., Tamm, E. R., Suter, U., and Wegner, M. (2011) Sox10 is required for Schwann-cell homeostasis and myelin maintenance in the adult peripheral nerve. *Glia* **59,** 1022–1032
35. Zimmermann, K., Hein, A., Hager, U., Kaczmarek, J. S., Turnquist, B. P., Clapham, D. E., and Reeh, P. W. (2009) Phenotyping sensory nerve endings *in vitro* in the mouse. *Nat. Protoc.* **4,** 174–196
36. Xu, H., Delling, M., Jun, J. C., and Clapham, D. E. (2006) Oregano, thyme and clove-derived flavors and skin sensitizers activate specific TRP channels. *Nat. Neurosci.* **9,** 628–635
37. Doerner, J. F., Gisselmann, G., Hatt, H., and Wetzel, C. H. (2007) Transient receptor potential channel A1 is directly gated by calcium ions. *J. Biol. Chem.* **282,** 13180–13189
38. Wang, Y. Y., Chang, R. B., Waters, H. N., McKemy, D. D., and Liman, E. R. (2008) The nociceptor ion channel TRPA1 is potentiated and inactivated by permeating calcium ions. *J. Biol. Chem.* **283,** 32691–32703
39. Everaerts, W., Gees, M., Alpizar, Y. A., Farre, R., Leten, C., Apetrei, A., Dewachter, I., van Leuven, F., Vennekens, R., De Ridder, D., Nilius, B., Voets, T., and Talavera, K. (2011) The capsaicin receptor TRPV1 is a crucial mediator of the noxious effects of mustard oil. *Curr. Biol.* **21,** 316–321

40. Ruparel, N. B., Patwardhan, A. M., Akopian, A. N., and Hargreaves, K. M. (2008) Homologous and heterologous desensitization of capsaicin and mustard oil responses utilize different cellular pathways in nociceptors. *Pain* **135,** 271–279
41. Bernardini, N., Neuhuber, W., Reeh, P. W., and Sauer, S. K. (2004) Morphological evidence for functional capsaicin receptor expression and calcitonin gene-related peptide exocytosis in isolated peripheral nerve axons of the mouse. *Neuroscience* **126,** 585–590
42. Kobayashi, K., Fukuoka, T., Obata, K., Yamanaka, H., Dai, Y., Tokunaga, A., and Noguchi, K. (2005) Distinct expression of TRPM8, TRPA1, and TRPV1 mRNAs in rat primary afferent neurons with Aδ/C-fibers and colocalization with trk receptors. *J. Comp. Neurol.* **493,** 596–606
43. Nassenstein, C., Kwong, K., Taylor-Clark, T., Kollarik, M., Macglashan, D. M., Braun, A., and Undem, B. J. (2008) Expression and function of the ion channel TRPA1 in vagal afferent nerves innervating mouse lungs. *J. Physiol.* **586,** 1595–1604
44. Taylor-Clark, T. E., McAlexander, M. A., Nassenstein, C., Sheardown, S. A., Wilson, S., Thornton, J., Carr, M. J., and Undem, B. J. (2008) Relative contributions of TRPA1 and TRPV1 channels in the activation of vagal bronchopulmonary C-fibres by the endogenous autacoid 4-oxononenal. *J. Physiol.* **586,** 3447–3459
45. Schmidt, M., Dubin, A. E., Petrus, M. J., Earley, T. J., and Patapoutian, A. (2009) Nociceptive signals induce trafficking of TRPA1 to the plasma membrane. *Neuron* **64,** 498–509
46. Douglas, W. W., and Ritchie, J. M. (1957) A technique for recording functional activity in specific groups of medullated and non-medullated fibres in whole nerve trunks. *J. Physiol.* **138,** 19–30
47. Weidner, C., Schmidt, R., Schmelz, M., Hilliges, M., Handwerker, H. O., and Torebjörk, H. E. (2000) Time course of post-excitatory effects separates afferent human C fibre classes. *J. Physiol.* **527,** 185–191
48. De Col, R., Messlinger, K., and Carr, R. W. (2008) Conduction velocity is regulated by sodium channel inactivation in unmyelinated axons innervating the rat cranial meninges. *J. Physiol.* **586,** 1089–1103
49. Bierhaus, A., Fleming, T., Stoyanov, S., Leffler, A., Babes, A., Neacsu, C., Sauer, S. K., Eberhardt, M., Schnölzer, M., Lasischka, F., Neuhuber, W. L., Kichko, T. I., Konrade, I., Elvert, R., Mier, W., Pirags, V., Lukic, I. K., Morcos, M., Dehmer, T., Rabbani, N., Thornalley, P. J., Edelstein, D., Nau, C., Forbes, J., Humpert, P. M., Schwaninger, M., Ziegler, D., Stern, D. M., Cooper, M. E., Haberkorn, U., Brownlee, M., Reeh, P. W., and Nawroth, P. P. (2012) Methylglyoxal modification of $Na_v1.8$ facilitates nociceptive neuron firing and causes hyperalgesia in diabetic neuropathy. *Nat. Med.* **18,** 926–933
50. del Camino, D., Murphy, S., Heiry, M., Barrett, L. B., Earley, T. J., Cook, C. A., Petrus, M. J., Zhao, M., D'Amours, M., Deering, N., Brenner, G. J., Costigan, M., Hayward, N. J., Chong, J. A., Fanger, C. M., Woolf, C. J., Patapoutian, A., and Moran, M. M. (2010) TRPA1 contributes to cold hypersensitivity. *J. Neurosci.* **30,** 15165–15174
51. Koop, D. R., Morgan, E. T., Tarr, G. E., and Coon, M. J. (1982) Purification and characterization of a unique isozyme of cytochrome P-450 from liver microsomes of ethanol-treated rabbits. *J. Biol. Chem.* **257,** 8472–8480
52. Lyles, G. A., and Chalmers, J. (1992) The metabolism of aminoacetone to methylglyoxal by semicarbazide-sensitive amine oxidase in human umbilical artery. *Biochem. Pharmacol.* **43,** 1409–1414
53. Nemet, I., Turk, Z., Duvnjak, L., Car, N., and Varga-Defterdarović, L. (2005) Humoral methylglyoxal level reflects glycemic fluctuation. *Clin. Biochem.* **38,** 379–383
54. Beisswenger, P. J., Howell, S. K., O'Dell, R. M., Wood, M. E., Touchette, A. D., and Szwergold, B. S. (2001) α-Dicarbonyls increase in the postprandial period and reflect the degree of hyperglycemia. *Diabetes Care* **24,** 726–732
55. Thornalley, P. J. (1993) The glyoxalase system in health and disease. *Mol. Aspects Med.* **14,** 287–371
56. Thornalley, P. J., Edwards, L. G., Kang, Y., Wyatt, C., Davies, N., Ladan, M. J., and Double, J. (1996) Antitumour activity of *S-p*-bromobenzylglutathione cyclopentyl diester *in vitro* and *in vivo*. Inhibition of glyoxalase I and induction of apoptosis. *Biochem. Pharmacol.* **51,** 1365–1372
57. Krizner, H. E., De Haan, D. O., and Kua, J. (2009) Thermodynamics and kinetics of methylglyoxal dimer formation: a computational study. *J. Phys. Chem. A* **113,** 6994–7001
58. Axson, J. L., Takahashi, K., De Haan, D. O., and Vaida, V. (2010) Gas-phase water-mediated equilibrium between methylglyoxal and its geminal diol. *Proc. Natl. Acad. Sci. U.S.A.* **107,** 6687–6692
59. Kikuchi, S., Shinpo, K., Moriwaka, F., Makita, Z., Miyata, T., and Tashiro, K. (1999) Neurotoxicity of methylglyoxal and 3-deoxyglucosone on cultured cortical neurons: synergism between glycation and oxidative stress, possibly involved in neurodegenerative diseases. *J. Neurosci. Res.* **57,** 280–289
60. Di Loreto, S., Caracciolo, V., Colafarina, S., Sebastiani, P., Gasbarri, A., and Amicarelli, F. (2004) Methylglyoxal induces oxidative stress-dependent cell injury and up-regulation of interleukin-1β and nerve growth factor in cultured hippocampal neuronal cells. *Brain Res.* **1006,** 157–167
61. Fukunaga, M., Miyata, S., Liu, B. F., Miyazaki, H., Hirota, Y., Higo, S., Hamada, Y., Ueyama, S., and Kasuga, M. (2004) Methylglyoxal induces apoptosis through activation of p38 MAPK in rat Schwann cells. *Biochem. Biophys. Res. Commun.* **320,** 689–695
62. Leppäluoto, J., and Ruskoaho, H. (1992) Endothelin peptides: biological activities, cellular signalling and clinical significance. *Ann. Med.* **24,** 153–161
63. Ergul, A. (2011) Endothelin-1 and diabetic complications: focus on the vasculature. *Pharmacol. Res.* **63,** 477–482
64. Dhaun, N., Goddard, J., and Webb, D. J. (2006) The endothelin system and its antagonism in chronic kidney disease. *J. Am. Soc. Nephrol.* **17,** 943–955
65. Plant, T. D., Zöllner, C., Kepura, F., Mousa, S. S., Eichhorst, J., Schaefer, M., Furkert, J., Stein, C., and Oksche, A. (2007) Endothelin potentiates TRPV1 via ETA receptor-mediated activation of protein kinase C. *Mol. Pain* **3,** 35
66. Namer, B., Hilliges, M., Orstavik, K., Schmidt, R., Weidner, C., Torebjörk, E., Handwerker, H., and Schmelz, M. (2008) Endothelin 1 activates and sensitizes human C-nociceptors. *Pain* **137,** 41–49
67. Toyokuni, S., Yamada, S., Kashima, M., Ihara, Y., Yamada, Y., Tanaka, T., Hiai, H., Seino, Y., and Uchida, K. (2000) Serum 4-hydroxy-2-nonenal-modified albumin is elevated in patients with type 2 diabetes mellitus. *Antioxid. Redox Signal.* **2,** 681–685
68. Traverso, N., Menini, S., Cosso, L., Odetti, P., Albano, E., Pronzato, M. A., and Marinari, U. M. (1998) Immunological evidence for increased oxidative stress in diabetic rats. *Diabetologia* **41,** 265–270
69. Pabbidi, R. M., Yu, S. Q., Peng, S., Khardori, R., Pauza, M. E., and Premkumar, L. S. (2008) Influence of TRPV1 on diabetes-induced alterations in thermal pain sensitivity. *Mol. Pain* **4,** 9
70. Hong, S., and Wiley, J. W. (2005) Early painful diabetic neuropathy is associated with differential changes in the expression and function of vanilloid receptor 1. *J. Biol. Chem.* **280,** 618–627
71. Messinger, R. B., Naik, A. K., Jagodic, M. M., Nelson, M. T., Lee, W. Y., Choe, W. J., Orestes, P., Latham, J. R., Todorovic, S. M., and Jevtovic-Todorovic, V. (2009) *In vivo* silencing of the $Ca_V3.2$ T-type calcium channels in sensory neurons alleviates hyperalgesia in rats with streptozocin-induced diabetic neuropathy. *Pain* **145,** 184–195
72. Jagodic, M. M., Pathirathna, S., Nelson, M. T., Mancuso, S., Joksovic, P. M., Rosenberg, E. R., Bayliss, D. A., Jevtovic-Todorovic, V., and Todorovic, S. M. (2007) Cell-specific alterations of T-type calcium current in painful diabetic neuropathy enhance excitability of sensory neurons. *J. Neurosci.* **27,** 3305–3316
73. Misawa, S., Sakurai, K., Shibuya, K., Isose, S., Kanai, K., Ogino, J., Ishikawa, K., and Kuwabara, S. (2009) Neuropathic pain is associated with increased nodal persistent Na^+ currents in human diabetic neuropathy. *J. Peripher. Nerv. Syst.* **14,** 279–284
74. Hong, S., Morrow, T. J., Paulson, P. E., Isom, L. L., and Wiley, J. W. (2004) Early painful diabetic neuropathy is associated with differential changes in tetrodotoxin-sensitive and -resistant sodium channels in dorsal root ganglion neurons in the rat. *J. Biol. Chem.* **279,** 29341–29350
75. de Arriba, S. G., Krügel, U., Regenthal, R., Vissiennon, Z., Verdaguer, E., Lewerenz, A., García-Jordá, E., Pallas, M., Camins, A., Münch, G., Nieber, K., and Allgaier, C. (2006) Carbonyl stress and NMDA receptor activation contribute to methylglyoxal neurotoxicity. *Free Radic. Biol. Med.* **40,** 779–790
76. Cook, L. J., Davies, J., Yates, A. P., Elliott, A. C., Lovell, J., Joule, J. A., Pemberton, P., Thornalley, P. J., and Best, L. (1998) Effects of methylg-

lyoxal on rat pancreatic β-cells. *Biochem. Pharmacol.* **55,** 1361–1367
77. Foulkes, T., and Wood, J. N. (2007) Mechanisms of cold pain. *Channels* **1,** 154–160
78. Obata, K., Katsura, H., Mizushima, T., Yamanaka, H., Kobayashi, K., Dai, Y., Fukuoka, T., Tokunaga, A., Tominaga, M., and Noguchi, K. (2005) TRPA1 induced in sensory neurons contributes to cold hyperalgesia after inflammation and nerve injury. *J. Clin. Investig.* **115,** 2393–2401
79. Kwan, K. Y., Glazer, J. M., Corey, D. P., Rice, F. L., and Stucky, C. L. (2009) TRPA1 modulates mechanotransduction in cutaneous sensory neurons. *J. Neurosci.* **29,** 4808–4819
80. Krämer, H. H., Rolke, R., Bickel, A., and Birklein, F. (2004) Thermal thresholds predict painfulness of diabetic neuropathies. *Diabetes Care* **27,** 2386–2391
81. Scott, A. R., Bennett, T., and Macdonald, I. A. (1987) Diabetes mellitus and thermoregulation. *Can. J. Physiol. Pharmacol.* **65,** 1365–1376
82. Courteix, C., Eschalier, A., and Lavarenne, J. (1993) Streptozocin-induced diabetic rats: behavioural evidence for a model of chronic pain. *Pain* **53,** 81–88
83. Talbot, S., Chahmi, E., Dias, J. P., and Couture, R. (2010) Key role for spinal dorsal horn microglial kinin B1 receptor in early diabetic pain neuropathy. *J. Neuroinflammation* **7,** 36
84. Ji, G., Zhou, S., and Carlton, S. M. (2008) Intact Aδ-fibers up-regulate transient receptor potential A1 and contribute to cold hypersensitivity in neuropathic rats. *Neuroscience* **154,** 1054–1066
85. Shin, J. B., Martinez-Salgado, C., Heppenstall, P. A., and Lewin, G. R. (2003) A T-type calcium channel required for normal function of a mammalian mechanoreceptor. *Nat. Neurosci.* **6,** 724–730
86. Wang, R., and Lewin, G. R. (2011) The Cav3.2 T-type calcium channel regulates temporal coding in mouse mechanoreceptors. *J. Physiol.* **589,** 2229–2243
87. Dubreuil, A. S., Boukhaddaoui, H., Desmadryl, G., Martinez-Salgado, C., Moshourab, R., Lewin, G. R., Carroll, P., Valmier, J., and Scamps, F. (2004) Role of T-type calcium current in identified D-hair mechanoreceptor neurons studied *in vitro*. *J. Neurosci.* **24,** 8480–8484
88. Khan, G. M., Chen, S. R., and Pan, H. L. (2002) Role of primary afferent nerves in allodynia caused by diabetic neuropathy in rats. *Neuroscience* **114,** 291–299
89. Jack, M. M., Ryals, J. M., and Wright, D. E. (2011) Characterisation of glyoxalase I in a streptozocin-induced mouse model of diabetes with painful and insensate neuropathy. *Diabetologia* **54,** 2174–2182
90. Wang, L., Cvetkov, T. L., Chance, M. R., and Moiseenkova-Bell, V. Y. (2012) *J. Biol. Chem.* **287,** 6169–6176